Uphill Energy Trapping by Reaction Center in Bacterial Photosynthesis: Charge Separation Unistep from Antenna Excitation, Virtually Mediated by Special-Pair Excitation

Hitoshi Sumi*

Institute of Materials Science, University of Tsukuba, Tsukuba 305-8573, Japan

Received: July 24, 2002; In Final Form: September 30, 2002

In the primary process of photosynthesis, energy of the electronic excited state, A*, in the core antenna is trapped by the reaction center into a state, B, of charge separation between pigments therein. This energy-trapping process is mediated by the excited state, P*, of the special pair of chlorophylls or bacteriochlorophylls in the reaction center. Energy transfer from A* to P* has been reported to be uphill with an excitation-energy difference, for example, amounting to about 200 and 350−400 cm^{-1} in *Rhodobacter (Rb.) sphaeroides* and *Rhodopseudomonas (Rps.) viridis*, respectively, in purple bacteria. The rate constant of this energy-trapping process was calculated with special attention to these species, reproducing observed data in the whole temperature range. At physiological temperatures, this process proceeds by the ordinary sequential mechanism, in which the second step from P* to B takes place after thermalization of phonons at P*, in both species. The uphill excitation-energy difference in the first step from A* to P* is blurred out by thermal activation with nearly uniform rate constants of about $(50\ ps)^{-1}$ for the energy trapping at room temperature. In *Rb. sphaeroides*, P* is thermally (i.e., in the free energy) lower than A* by about 50 cm^{-1} because of reorganizing relaxation of the medium in association with excitation of pigments. Correspondingly therein, the energy-trapping process is determined by the ordinary sequential mechanism at all temperatures. In *Rps. viridis*, P* is thermally still higher than A* by about 150 cm^{-1}. Correspondingly, below about 50 K therein, the energy-trapping process changes to the superexchange mechanism in which mediation at P* takes place as a quantum-mechanical virtual process without real population at P*. This mechanism resolves a serious difficulty that the observed data and the expectation from the ordinary sequential mechanism deviate to an astronomical extent at low temperatures in *Rps. viridis*.

I. Introduction

In the primary process of photosynthesis, solar energy is first harvested by the antenna system as electronic excitations of pigments. They are transferred among pigments toward the reaction center (RC) and trapped by it. The RC is a transmembrane protein−pigment complex, and the energy trapped by it is converted to an electrochemical energy by charge separation against the electrostatic-potential gradient within the RC. Research on such initial electronic processes of photosynthesis has been explosively developed in these 15 years.[1] Such a remarkable era was opened in 1984 by the first clarification of the three-dimensional structure of the RC from photosynthetic purple bacteria.[2] Research was further stimulated in 1995 by that of a transmembrane protein−pigment complex, LH2, in the peripheral antenna system also for purple bacteria.[3] LH2s surround the core−antenna protein−pigment complex, LH1, which encloses the RC. These investigations have clarified that pigments in the RC constitute two strands, which are in the 2-fold rotational symmetry. Pigments in LH2 constitute a ring with the 9- or 8-fold rotational symmetry depending on species. In some species of purple bacteria, there exists a third type of light-harvesting complex, LH3, outside a region of LH2s.[4] It was clarified very recently (in 2001) that LH3 has a ring structure with the same rotational symmetry as LH2.[5]

Photosynthesis is the ultimate energy source for all creatures on Earth. Accordingly, many people have been attracted by the finding that organisms participating in photosynthesis have beautiful structures with such high symmetries. It attracted not only biologists but also both chemists and physicists, letting them imagine that principles underlying the mystery of life should also be beautiful.

It was shown also for purple bacteria that pigments in LH1 constitute a ring with the sixteen-fold rotational symmetry,[6] and it attracted many people. In this case, the structure was determined from two-dimensional crystals. These features have not been settled yet, however, because it seems that LH1 has a complete ring structure only when it is reconstituted from detergent-solubilized protein complexes.[7] It has been shown, in fact, as an image of electron microscopy that LH1 enclosing the RC in the intact membrane has a C-shaped open structure with a cut of about one-fourth the whole ring under certain conditions.[8]

Structure determinations mentioned above have greatly promoted our understanding of photosynthesis as a function. The energy trapping begins with excitation transfer from the antenna system to the (so-called) special pair (P) of bacteriochlorophylls in bacterial photosynthesis (alternatively, to that of chlorophylls in higher plants, algae, and cyanobacteria) in the RC.[1,2] The excitation of P is very rapidly converted to a state of initial charge separation along one of the pigment strains within the RC by transferring an electron to the primary acceptor, which is bacteriopheophytin in purple bacteria. The distance between P and the primary acceptor is so large (∼17 Å in purple bacteria) that the electron transfer from P to the

* Fax: +81 (298) 55-7440. E-mail: sumi@ims.tsukuba.ac.jp.

10.1021/jp021716e CCC: $22.00
Published on Web 12/03/2002

primary acceptor is mediated stepwise by a pigment (B) located between them.[9] Accordingly, the initial charge-separated state produced in the RC is P^+B^-, and it is produced in ~3 ps after excitation of P in purple bacteria, where B is a bacteriochlorophyll monomer.

Excitations of antenna pigments are transferred from LH3 to LH2 and from LH2 to LH1 toward the RC in purple bacteria. Their excitation energies are arranged so as to decrease from LH3 toward LH2 and from LH2 toward LH1.[10] This situation is called the funnel structure, along which an electronic excitation flows down toward its central sink as water does along a funnel. Curiously, however, the excitation energies rise from LH1 to P.[11] The uphill excitation-energy difference, ΔE, amounts to ~200 cm^{-1} in *Rhodobacter* (*Rb.*) *sphaeroides* in purple non-sulfur bacteria, that is, to a value comparable to the thermal energy of ~210 cm^{-1} at room temperature.[12] In *Rhodopseudomonas* (*Rps.*) *viridis*, ΔE is considerably larger than the thermal energy, amounting to ~350−400 cm^{-1}.[13] Amounting to ~430 cm^{-1}, it becomes much larger than the thermal energy in a recently isolated species of purple sulfur bacteria, provisionally called strain 970.[14] Nevertheless, the rate constant for excitation-energy trapping from LH1 by the RC is nearly uniform among these species at room temperature with magnitudes of $(\sim 45.7\ ps)^{-1}$ in *Rb. sphaeroides*,[15] $(\sim 50\ ps)^{-1}$ in *Rps. viridis*,[16] and $(\sim 65\ ps)^{-1}$ in strain 970.[14] These magnitudes decrease only very gradually with ΔE despite its considerable increase in the scale of the thermal energy. Such an uphill energy transfer in the energy-trapping process has widely been known also in other species in bacterial photosynthesis,[12,13b,16a,17] and both the origin and the meaning of such uniformity in the rate constant have not well been rationalized.[14,17b,17f]

Excitation of the antenna system, produced by harvesting the solar energy, rapidly reaches its lowest-energy state (LH1*) of so-called red pigments in LH1 within ~10 ps at room temperature.[11] As soon as the energy is transferred to the excited state (P*) of P in the RC, it is almost simultaneously converted into the initial charge-separated state P^+B^- within the RC. It is this composite process that has been observed as excitation-energy trapping from the antenna system by the RC, taking about dozens of picosecond as mentioned above. This process is rate-limiting in the whole primary process of solar-energy harvesting and fixation.[11,18] Biological organisms have been adjusted in the course of evolution so as to function most effectively in a given environment. We can infer, accordingly, that it would be a result of evolution that the time constant of the excitation-energy trapping by the RC has been adjusted so as to be nearly uniform at room temperature despite considerable variations in ΔE among different species. It will be shown in the present work that such an adjustment has been accomplished by utilizing the appreciable width in the absorption peak of P together with the thermal energy at room temperature.

It is easily expected that such an adjustment for overcoming the uphill excitation-energy transfer will break down at low temperatures because both the absorption width of P* and the thermal energy decrease. In *Rb. sphaeroides*, on the contrary, the rate constant increases to $(35-45\ ps)^{-1}$ at 77−177 K from $(\sim 45.7\ ps)^{-1}$ at room temperature,[17a] although its increase is slight. In *Rps. viridis*, it considerably decreases to $(\sim 1.3\ ns)^{-1}$ at 6 K from $(\sim 50\ ps)^{-1}$ at room temperature.[13b] The excitation-energy difference ΔE from LH1 to P mentioned before represents the increase in the absorption-peak energy from LH1* to P*. It deviates from the corresponding increase in the free energy, ΔG, because of reorganizing relaxation of the surrounding medium in association with electronic excitation or deexcitation of pigments. Because the excitation-energy transfer from LH1* to P* is much slower than the formation of the initial charge-separated state from P* within the RC, the former should limit the rate constant k of the excitation-energy trapping by the RC. Therefore, the temperature (T) dependence of k should be stronger than that of $\exp(-\Delta G/(k_B T))$ as long as $\Delta G > 0$ because its thermal-activation energy is larger than ΔG, as explained in Appendix A in more detail. The temperature dependence of k in *Rb. sphaeroides*, mentioned above, seems to be indicating a case that ΔG is either negative or much smaller than $k_B T$ for 77 K even if $\Delta G > 0$, although $\Delta E \approx 200$ cm^{-1}. This is because only in such cases the temperature dependence of k can become controlled by that of its preexponential factor, which weakly decreases with temperature, as also explained in Appendix A. In *Rps. viridis*, ΔG has been estimated to be ~150 cm^{-1} although $\Delta E \approx 350-400$ cm^{-1}, taking appropriate account of the energy of the reorganization mentioned above.[11] With this value of ΔG, the ratio of $\exp(-\Delta G/(k_B T))$ between 6 and 300 K is $\sim 4.5 \times 10^{-16}$. The theoretical value of the ratio of k must be smaller than this ratio, as shown in eq A.1 of Appendix A, while the observed ratio of k between 6 and 300 K is only ~0.038. Therefore, there exists an astronomical deviation, larger than the order of 10^{14}, between theory and experiment. Various difficulties manifest themselves, reflecting originally this astronomical deviation, as have been noted in vague fashions in the literature.[18]

The rate-constant value of $(\sim 1.3\ ns)^{-1}$ at 6 K in *Rps. viridis* was obtained by measuring the quantum yield of charge-separated-state formation in the RC by core−antenna excitation.[13b] Therefore, this value represents the speed of the global decay in the number of LH1* by the charge-separated-state formation as the reaction. Therefore, this value cannot be attributed to a small portion of LH1−RC complexes with ΔG values favorable for the reaction in their inhomogeneous distribution, and this value must be regarded as an average rate constant.

The aim of the present work is to understand the meaning of the uphill energy transfer from LH1* to P* in the excitation-energy trapping by the RC in purple bacteria. To be more concrete, first we will reproduce theoretically the observed near uniformity in k at room temperature despite such a wide variation in ΔE. Second, we will rationalize, from the standpoint of the average rate constant, the serious deviation of the observed data from the conventional theory at low temperatures in *Rps. viridis*. In this context, it will be pointed out that the state of P* in the RC becomes a virtual intermediate state in quantum mechanics at low temperatures, connecting the state of LH1* with the initial charge-separated state P^+B^- in the RC by the superexchange mechanism,[19] the concept of which was originally introduced in magnetism. The state of LH1* in the antenna system is unistep converted to the initial charge-separated state P^+B^- in the RC without real population at the intermediate state P* at low temperatures in *Rps. viridis*. Such a superexchange virtual mediation by P* has already been speculated for heliobacterium *Heliobacillus mobilis* without rationalization.[17e] The present work puts this mechanism on a sound basis, presenting a concrete calculation. It will be performed for *Rb. sphaeroides* and *Rps. viridis* in purple bacteria because many physical parameters have been known for them as a result of accumulation of various investigations.

In *Rps. viridis*, mediation by P* in the excitation-energy trapping by the RC is sequential at room temperature with P* really realized, but it becomes superexchange at low temperatures. To reproduce the whole temperature dependence of the

observed rate constant k, therefore, we need a unified treatment between the sequential and the superexchange mediation. Such a theory has been presented by Sumi and Kakitani as an analytic formula of the rate constant for electron transfer mediated by a midway molecule. In this theory, each one of these mechanisms can be justified only in a limiting case of the general situation in which the process of electron-transfer mediated by a midway molecule is described as a single process as a whole. Originally, it was presented to rationalize the temperature dependence of electron transfer from P* to bacteriopheophytin mediated by the bacteriochlorophyll monomer B within the RC of purple bacteria.[20] Experimentally, this process has been attributed to the sequential process in which the initial charge-separated state P^+B^- is really realized in the course of the mediation, as mentioned before. This situation arises mainly because the energy position of the intermediate state is lower than the initial state P* by about several hundred wavenumbers in the organism of wild type. The superexchange mediation by the intermediate state easily appears at low temperatures when its energy position is slightly raised artificially by about several hundred wavenumbers, as described theoretically in ref 20b in agreement with observed data. The present work employs the analytic formula in ref 20b with modifications appropriate for the present process.

The state LH1* of so-called red pigments in LH1 gives the lowest excitation of the whole aggregate of bacteriochlorophylls in LH1.[21] Experiments of excitation-energy trapping by the RC are usually triggered by direct excitation of only the state of LH1* in LH1. In this situation, we consider it worthwhile to calculate the rate constant of excitation-energy trapping by the RC only from the state of LH1* in LH1. This approach seems justified also by a fact that interaction with phonons is very weak at LH1* because the corresponding excitation is delocalized over many bacteriochlorophylls and consequently has very weak interaction with distortions of the surrounding medium.[21] Subject to broadening, optical absorption of LH1* has been submerged in the low-energy tail of the absorption peak of LH1 the main part of which is given by the second-lowest excited state of LH1 located $\sim$120 cm^{-1} above the lowest excited state.[21b] If excitation-energy trapping to the RC takes place from the thermally equilibrated population over various excited states of LH1, the initial population must include both the lowest and the second-lowest excited states at least at room temperature where $k_BT \approx 210$ cm^{-1}. To pursue that approach, we must know the excitonic structure in LH1 in advance. To know it, the three-dimensional structure of LH1 must have been clarified in a form of complex with the RC. Unfortunately, however, the structure of LH1 has been inferred from LH1s reconstituted from detergent-solubilized protein complexes.[6,7] It has been shown by electron microscopy that the structure of LH1 thus reconstructed seems different in essential points from that in an LH1−RC complex in the intact membrane,[8] as pointed out earlier. In this situation, it seems unrealistic at present to pursue the latter approach, although it is also important.

The plan of the present article is as follows. The applicability of the theory in ref 20 after appropriate modifications is explained in section II. Setting of parameters is made in section III for calculation of the rate constant of the excitation-energy trapping as a single process from the state of red pigments LH1* into charge separation in the RC. Results of numerical calculation are shown in section IV for understanding and analyzing the observed rate constant in *Rb. sphaeroides* and *Rps. viridis*. Remaining discussions are put in section V, together with predictions on the temperature dependence of the rate constant in artificially modified systems. Summaries are given in section VI.

People not interested in the formulation and its associated parameter setting can directly proceed from here to section IV, skipping sections II and III.

II. Excitation-Energy Trapping from LH1* to P^+B^- Mediated by P*

The initial, the intermediate, and the final states in the excitation-energy trapping are respectively represented by electronic states

$$|d\rangle \quad \text{for} \quad \text{LH1*·P·B}, \quad |m\rangle \quad \text{for} \quad \text{LH1·P*·B}, \quad \text{and} \quad |a\rangle \quad \text{for} \quad \text{LH1·P}^+\text{·B}^- \tag{2.1}$$

At each state, the surrounding medium reorganizes as a result of its interaction with electrons within a protein−pigment complex. At the initial state $|d\rangle$ in which LH1 is in its lowest excited state LH1*, we consider approximately that reorganization of the medium takes place only around LH1. Let us express the energy of the reorganization by λ_d. In reality, however, λ_d has been observed to be very small, at most on the order of several cm^{-1}, reflecting that interaction with phonons is very small at LH1*,[21] as noted in section I. Nevertheless, λ_d is retained for a while, from a necessity to make adaptation of the formalism in ref 20 unambiguous. At the intermediate state $|m\rangle$ in which only the special pair P of bacteriochlorophylls in the RC is excited, we consider similarly that reorganization of the medium takes place only around P. Let us express the energy of the reorganization by $\lambda_m^{(d)}$. At the final state, charges are separated between P and the monomeric bacteriochlorophyll B in the RC, and we consider similarly that the medium is reorganized only around both P and B. Associated reorganization energies are written as $\lambda_m^{(a)}$ and λ_a, respectively.

Reorganization energies are measured in reference to the configuration of the medium reorganized at $|m\rangle$, to make the comparison with the formulation in ref 20b straightforward in their definition. Excitation-energy transfer to $|m\rangle$ from $|d\rangle$ releases reorganization of the medium around both LH1 and P in this reference frame. The total energy of reorganization in response to this electronic transition is associated with deexcitation of LH1* and excitation of P, being given by $\lambda_d + \lambda_m^{(d)}$. Charge separation to $|a\rangle$ from $|m\rangle$ induces reorganization in both P and B in this reference frame. The total energy of reorganization in response to this electronic transition is associated with oxidation of (i.e., electron removal from) P* to P^+ and reduction of (i.e., electron insertion to) B into B^-, being given by $\lambda_m^{(a)} + \lambda_a$. In charge separation to $|a\rangle$ unistep from $|d\rangle$, reorganization is induced in response to both deexcitation of LH1* and formation of the charge-separated state $P^+\cdot B^-$ from P·B. Seen from this reference frame, P and P^+ are regarded as formed from P* by deexcitation and by oxidation, respectively. The reorganization energy associated with oxidation of P* has been written as $\lambda_m^{(a)}$, while that associated with its deexcitation has been written as $\lambda_m^{(d)}$. Let us write the reorganization energy associated with oxidation of P as $\lambda_m^{(a)} + \lambda_m^{(d)} - 2\lambda_m$. The last term therein arises from correlation between reorganizing-distortion modes in response to deexcitation of P* and those in response to its oxidation. Although the explicit expression of λ_m is given in Appendix B, it becomes either positive or negative depending on whether reorganizing-distortion modes common between them distort on the average in the same or opposite

direction, respectively, in response to deexcitation and to oxidation of P*. In the former case, the reorganizing-distortion modes common between them remain distorted in the same direction on the average before and after oxidation of P, while the modes are distorted in the opposite direction on the average in the latter case. Even if λ_m is positive, $\lambda_m^{(a)} + \lambda_m^{(d)} - 2\lambda_m$ is positive as a whole, as shown in Appendix B. Thus, the total reorganization energy associated with charge separation to $|a\rangle$ unistep from $|d\rangle$ is given by $\lambda_a + \lambda_m^{(a)} + \lambda_m^{(d)} - 2\lambda_m + \lambda_d$, supplemented by the reorganization energies λ_d and λ_a associated with deexcitation of LH1* and reduction of B, respectively.

When ΔG_m represents the free energy at $|m\rangle$ measured from that at $|d\rangle$, the thermal activation energy for excitation-energy transfer to $|m\rangle$ from $|d\rangle$ is given by

$$\Delta G_{m,d}^* = \frac{1}{4}(\Delta G_m + \lambda_m^{(d)} + \lambda_d)^2/(\lambda_m^{(d)} + \lambda_d) \qquad (2.2)$$

from the Marcus relation.[22] Similarly, when ΔG_a represents the free energy at $|a\rangle$ measured from $|d\rangle$, the thermal activation energy for charge separation to $|a\rangle$ from $|m\rangle$ is given by

$$\Delta G_{a,m}^* = \frac{1}{4}(\Delta G_a - \Delta G_m + \lambda_a + \lambda_m^{(a)})^2/(\lambda_a + \lambda_m^{(a)}) \quad (2.3)$$

The thermal activation energy for charge separation to $|a\rangle$ unistep from $|d\rangle$ is given by

$$\Delta G_{a,d}^* = \frac{1}{4}(\Delta G_a + \lambda_a + \lambda_m^{(a)} + \lambda_m^{(d)} - 2\lambda_m + \lambda_d)^2/(\lambda_a + \lambda_m^{(a)} + \lambda_m^{(d)} - 2\lambda_m + \lambda_d) \quad (2.4)$$

Interaction of an electron with distortions of the surrounding medium brings about not only its reorganization but also (both thermal and quantum-mechanical) fluctuations in the energy of the electron. The average squared amplitude of the fluctuations are expressed as D_d^2, $D_m^{(d)2}$, $D_m^{(a)2}$, and D_a^2 accompanied with the energies of reorganization of the medium, λ_d around LH1, $\lambda_m^{(d)}$ around P, $\lambda_m^{(a)}$ also around P, and λ_a around B, respectively. Their explicit expressions are given in Appendix C. As shown also therein and in general in ref 22, they can approximately be expressed as

$$D_d^2 = 2k_BT'\lambda_d, \quad D_m^{(d)2} = 2k_BT'\lambda_m^{(d)}, \quad D_m^{(a)2} = 2k_BT'\lambda_m^{(a)}, \quad \text{and} \quad D_a^2 = 2k_BT'\lambda_a \quad (2.5)$$

Here, T' represents an effective temperature determined in such a way that k_BT' gives the average squared amplitude in (both thermal and quantum-mechanical) fluctuations of phonons participating in the reorganization of the medium. When $\hbar\varpi$ represents the average energy quantum of such phonons, k_BT' can be approximated by[20b,22]

$$k_BT' = \frac{1}{2}\hbar\varpi \coth\left(\frac{1}{2}\hbar\varpi/(k_BT)\right) \qquad (2.6)$$

At high and low temperatures, k_BT' approaches

$$k_BT' \approx \begin{cases} k_BT \text{ for } k_BT \gg \hbar\varpi \\ \hbar\varpi/2 \text{ for } k_BT \ll \hbar\varpi \end{cases} \qquad (2.7)$$

This equation means that at high temperatures k_BT' approaches the average energy k_BT of a single oscillator determined by the equilipartition law of energy in classical mechanics while at low temperatures it approaches the quantum-mechanical energy of zero-point vibrations, $\hbar\varpi/2$, of the single oscillator with angular frequency ϖ.

In association with oxidation of P to P^+, the energy of reorganization of the medium around P is given by $\lambda_m^{(a)} + \lambda_m^{(d)} - 2\lambda_m$, and it is accompanied by fluctuations in the energy difference between P and P^+. As shown in Appendix C, when the average squared amplitude of the fluctuations is written as $D_m^{(a)2} + D_m^{(d)2} - 2D_m^2$, the last term therein can similarly be approximated by

$$D_m^2 = 2k_BT'\lambda_m \qquad (2.8)$$

with an expediency that D_m^2 is negative when λ_m is negative.

In discrimination of whether the charge separation to $|a\rangle$ from $|d\rangle$ is unistep via virtual mediation at $|m\rangle$ or sequential with real population at $|m\rangle$, a decisive role is played by the dephasing-thermalization time, τ_m, of phonons participating in the reorganization of the medium at $|m\rangle$.[20,23] Here, $1/\tau_m$ can be estimated by the average width in frequency dispersion of such phonons around P, as shown in Appendix B. To be more concrete, in response to a situation that reorganizing motions of the medium associated with deexcitation of P* and those associated with its oxidation correlate with energy λ_m around P, time evolution in the former induces that in the latter. The correlation evolves with time τ as a time-dependent correlation energy, $\lambda_m(\tau)$, after a switch of excitation-energy transfer to $|m\rangle$ from $|d\rangle$ at $\tau = 0$. Such a quantum-mechanical evolution of the medium is accompanied by a time-dependent broadening, $D_m(\tau)^2$, as shown also in Appendix C. Both $\lambda_m(\tau)$ and $D_m(\tau)^2$ decay to zero in the limit of $\tau \gg \tau_m$, starting from λ_m and D_m^2, respectively, at $\tau = 0$. Such a time evolution can be approximated by[20b]

$$\lambda_m(\tau) = \lambda_m \exp(-\tau^2/\tau_m^2) \quad \text{and} \quad D_m(\tau)^2 = D_m^2 \exp(-\tau^2/\tau_m^2) \quad (2.9)$$

In response to a switch of excitation-energy transfer to $|m\rangle$ from $|d\rangle$ at time zero, moreover, reorganization of the medium evolves quantum mechanically with time t (≥ 0) until it is released around both P and LH1, measured from the configuration of the medium relaxed at $|m\rangle$. The time evolution is expressed by the time-dependent reorganization energies, $\lambda_m^{(d)}(t)$ around P and $\lambda_d(t)$ around LH1. Under a simplification that decay of them can be described by the same dephasing-thermalization time τ_m, they should approach zero in the limit of $t \gg \tau_m$, starting from $\lambda_m^{(d)}$ and λ_d, respectively, at $t = 0$. Therefore, they can approximately be expressed, similarly to eq 2.9,[20b] as

$$\lambda_m^{(d)}(t) = \lambda_m^{(d)} \exp(-t^2/\tau_m^2) \quad \text{and} \quad \lambda_d(t) = \lambda_d \exp(-t^2/\tau_m^2) \qquad (2.10)$$

As mentioned before, we employ the analytic formula of the rate constant for a similar problem of electron transfer in ref 20b with some modifications. It has been taken into account therein that an electron interacts in B not only with medium distortions contributing to the reorganization energy, λ_a, but also with intramolecular phonons of a large energy quantum, $\hbar\omega_a$, with a reorganization energy $S_a\hbar\omega_a$. In this situation, the reorganization energy, λ_a, has been called the outersphere component while that $S_a\hbar\omega_a$ has been called the innersphere component with S_a called the Huang−Rhys factor.[22] In the analytic formula, phonons contributing to the outersphere reorganization by energies λ_d, $\lambda_m^{(d)}$, $\lambda_m^{(a)}$, and λ_a are treated in the semiclassical approximation.

With these quantities mentioned above, the rate constant $k_{a,d}$ for formation of the charge-separated state $|a\rangle$ from $|d\rangle$ mediated by $|m\rangle$ can be obtained from the analytic formula in ref 20b (to be more exact, eq 4.1 with eqs 5.17 and 5.25 therein) by replacements

$$\lambda_d \rightarrow \lambda_d + \lambda_m^{(d)} - \lambda_m, \quad \lambda_a \rightarrow \lambda_a + \lambda_m^{(a)} - \lambda_m,$$
$$\lambda_d(t) \rightarrow \lambda_d(t) + \lambda_m^{(d)}(t) - \lambda_m(t),$$
$$D_d{}^2 \rightarrow D_d{}^2 + D_m^{(d)2} - D_m{}^2, \quad \text{and}$$
$$D_a{}^2 \rightarrow D_a{}^2 + D_m^{(a)2} - D_m{}^2 \quad (2.11)$$

as shown in Appendix C. Inversely, the analytic formula in ref 20b corresponds to a case of $\lambda_m^{(d)} = \lambda_m^{(a)} = \lambda_m$, $\lambda_m^{(d)}(t) = \lambda_m(t)$, and $D_m^{(d)2} = D_m^{(a)2} = D_m{}^2$. With replacements in eq 2.11, we write

$$k_{a,d} = \int_0^\infty F(\tau)\, d\tau \quad (2.12)$$

as the analytic formula for the $k_{a,d}$ where $F(\tau)$ is a positive function shown in Appendix D. The integration variable τ on the right-hand side of eq 2.12 physically represents time spent at $|m\rangle$ after a quantum-mechanical virtual transition to $|m\rangle$ from $|d\rangle$ at $\tau = 0$. Then,

$$\exp(-\bar{\tau}_m{}^2/\tau_m{}^2) = 0.1 \quad \text{for} \quad \bar{\tau}_m \approx 1.52\tau_m \quad (2.13)$$

shows that reorganization of the medium at $|m\rangle$ has almost been completed at $\tau = \bar{\tau}_m$. Therefore, it is convenient to divide the τ integration in eq 2.12 into contributions before and after $\tau = \bar{\tau}_m$. As shown in eq 4.9 of ref 20b, this division enables us to cast eq 2.12 into

$$k_{a,d} \approx \int_0^{\bar{\tau}_m} F(\tau)\, d\tau + k_{a,d}^{(OS)} P_m \quad (2.14)$$

where P_m represents the survival probability of an electronic excitation at P* until time $\bar{\tau}_m$, given explicitly by eq D.11 in Appendix D or eq 4.6 in ref 20b. In the present problem, radiative decay can decrease P_m, but in reality, its probability can be neglected. The term $k_{a,d}^{(OS)}$ in eq 2.14 represents the rate constant for charge separation to $|a\rangle$ from $|d\rangle$ mediated by $|m\rangle$ in the ordinary sequential mechanism. In this mechanism, not only is the intermediate state $|m\rangle$ really populated but also the second transition to $|a\rangle$ from $|m\rangle$ takes place after thermalization of phonons at $|m\rangle$. Accordingly, the rate constant in this mechanism is given by

$$k_{a,d}^{(OS)} = 1/[k_{m,d}{}^{-1} + (k_{a,m}K_m)^{-1}] \quad (2.15)$$

a formula well-known in textbooks, naturally reached as eq 3.2 in the formulation of ref 20b. Here, $k_{m,d}$ and $k_{a,m}$ represent the rate constant for excitation transfer to $|m\rangle$ from $|d\rangle$ and electron transfer to $|a\rangle$ from $|m\rangle$, respectively, and K_m represents the equilibrium constant at $|m\rangle$ relative to $|d\rangle$ determined by the free energy ΔG_m at $|m\rangle$ relative to $|d\rangle$, as

$$K_m = \exp[-\Delta G_m/(k_B T)] \quad (2.16)$$

The first term on the right-hand side of eq 2.14 represents contributions to $k_{a,d}$ in the time region before $\bar{\tau}_m$ while phonons at $|m\rangle$ are not thermalized yet. Taking place in this time region are not only the charge separation to $|a\rangle$ unistep from $|d\rangle$ but also the hot sequential charge separation. In the former, charge separation to $|a\rangle$ from $|m\rangle$ takes place before loss of phase memories among phonons at $|m\rangle$ after a virtual excitation transfer to $|m\rangle$ from $|d\rangle$ at time $\tau = 0$. In the latter, it takes place after loss of phase memories among phonons at $|m\rangle$ but in the course of energetic thermalization of phonons therein after the excitation transfer to $|m\rangle$ from $|d\rangle$ at time $\tau = 0$. In reality, however, it has been known[23] and also explicitly shown in ref 20b that such dephasing and thermalization of phonons take place simultaneously with the same time constant, τ_m. Therefore, contributions to $k_{a,d}$ from the former and the latter cannot unambiguously be separated except in a special case. For example, the usual formula in the superexchange mechanism for the charge separation to $|a\rangle$ unistep from $|d\rangle$, given by $k_{a,d}^{(SX)}$ of eq 3.7 in ref 20b, can analytically be cast into eq 5.31 therein in the semiclassical approximation for phonons contributing to the outersphere reorganization. As noted in ref 20b, in fact, even this formula contains partially also contributions from the latter, that is, the hot sequential charge separation in the present problem.

In the situation mentioned above, it is reasonable to introduce only the degree of ordinary sequentiality, D_{OS}, as in ref 20b. Considering $F(\tau) > 0$ on the right-hand side of eq 2.14 for the rate constant $k_{a,d}$, it is given by the proportionality of the second term therein as

$$D_{OS} = (k_{a,d}^{(OS)}/k_{a,d})P_m \quad \text{with} \quad 0 < D_{OS} < 1 \quad (2.17)$$

Charge separation to $|a\rangle$ from $|d\rangle$ mediated by $|m\rangle$ proceeds by the ordinary sequential mechanism when $D_{OS} \gg 0.1$. On the other hand, the charge separation proceeds by the unistep superexchange mechanism as long as $k_{a,d} \approx k_{a,d}^{(SX)}$, when $D_{OS} \ll 1$.

III. Parameter Setting

The value of λ_d has been observed to be very small, at most on the order of several cm^{-1}, in *Rb. sphaeroides*,[21] as noted in section II. Therefore, it is neglected in the numerical calculation of $k_{a,d}$. Because $\lambda_m^{(d)}$ has also been observed in *Rb. sphaeroides*[24] to be $\sim$250 cm^{-1}, $\lambda^{(d)}{}_m$ is set at 250 cm^{-1} for *Rb. sphaeroides* and also for *Rps. viridis*. In ref 20b, such a setting of $\lambda_m^{(d)}$ common for both species was effective in reproducing theoretically both the temperature dependence and the magnitude of the rate constant for electron transfer from P* to bacteriopheophytin mediated by the reduced state B^- of the monomeric bacteriochlorophyll B in the RC. It seems reasonable to set $\lambda_m^{(a)}$ and λ_a at 250 and 350 cm^{-1}, respectively, also commonly for both species, because these values were also effective in the calculation in ref 20b.

Reorganization giving rise to $\lambda_m^{(d)}$ at P* has been known to be dominated by shrink in the distance between the two bacteriochlorophylls in P.[24] In the state of P^+, the positive charge is partially localized at one of the two bacteriochlorophylls to a significant extent.[25] This means that the distance between them should expand in response to oxidation of P* to P^+, giving rise to the reorganization energy $\lambda_m^{(a)}$. The distance also expands in response to deexcitation of P* to P. Accordingly, reorganizing-distortion modes in response to deexcitation of P* partially overlap with those in response to its oxidation, and the modes common between them distort on the average in the same direction in response to these electronic transitions. Accordingly, the distance between the two bacteriochlorophylls in P should remain expanded on the average in reference to that in P* before and after oxidation of P. This means that λ_m is positive. As shown in Appendix B, λ_m can be expressed as

$\lambda_m = g(\lambda_m^{(a)}\lambda_m^{(d)})^{1/2}$, where g represents the direction cosine between the two directions determined by the two sets of reorganizing distortions in the multidimensional phonon-coordinate space. Its absolute value $|g|$ is smaller than unity. Considering the large positive correlation between the two sets of modes, we set g at 0.7. The value of $k_{a,d}$ is not sensitive to the value of g except in the superexchange mediation at $|m\rangle$ for the unistep charge separation to $|a\rangle$ from $|d\rangle$. Intramolecular phonons participating in the innersphere reorganization have usually large energy quanta on the order of 1000 cm^{-1}. Therefore, they play an important role when the final state $|a\rangle$ is lower than either the initial state $|d\rangle$ or the intermediate state $|m\rangle$ by an energy larger than $\sim$1000 cm^{-1}.[22] In the present problem, these states are within an energy range smaller than $\sim$1000 cm^{-1}, as shown later. Accordingly, the Huang−Rhys factor S_a describing the coupling with such phonons is neglected in the present calculation.

The dephasing-thermalization time of phonons, τ_m, at $|m\rangle$ can be estimated by the inverse of the average width in frequency dispersion of phonons interacting with an electron, as mentioned before. The average energy quantum of such phonons has been denoted by $\hbar\varpi$. In both the antenna system and the RC, pigments are encompassed in proteins. It has been observed that vibrations of a protein have in general average energies of several dozens of cm^{-1}, extending to about 100 cm^{-1}.[24,26] As a typical example, therefore, let us take $\hbar\varpi$ at 50 cm^{-1} and τ_m at 0.3 ps, considering that the average width in phonon-energy dispersion is about 100 cm^{-1}. Such a rapid thermalization of protein distortions in the time region of 0.3 ps has in fact been observed in association with electron transfer in a blue-copper protein, plastocyanin, by direct time-domain measurements (as $\sim$0.36 ps in this case).[27] These values of $\hbar\varpi$ and τ_m were adopted also in the calculation in ref 20b, successfully reproducing the observed data on the initial charge separation from P* in the RC for both *Rb. sphaeroides* and *Rps. viridis*.

Free energies at $|m\rangle$ and $|a\rangle$ relative to $|d\rangle$ were written as ΔG_m and ΔG_a respectively. It has widely been accepted that $|a\rangle$ is thermally $\sim$450 cm^{-1} lower than $|m\rangle$ in *Rb. sphaeroides*.[9] Also for *Rps. viridis*, $\Delta G_m - \Delta G_a = \sim$450 cm^{-1} was effective in the calculation in ref 20b. Accordingly, it seems reasonable to adopt $\Delta G_m - \Delta G_a = 450$ cm^{-1} commonly for both species. Because ΔG_m has been estimated to be $\sim$150 cm^{-1} in *Rps. viridis*,[11] as mentioned in section I, let us take ΔG_m at 150 cm^{-1} for *Rps. viridis*. ΔG_m is lower by about $\lambda_d + \lambda_m^{(d)}$ ($\sim\lambda_m^{(d)}$) than the energy difference, ΔE, mentioned in section I, between optical absorption peaks of LH1* and P*. In *Rb. sphaeroides*, ΔE and $\lambda_m^{(d)}$ have been observed to be $\sim$200 and $\sim$250 cm^{-1}, respectively, as mentioned in section I and in this section. Accordingly, it seems reasonable to take ΔG_m at −50 cm^{-1} for *Rb. sphaeroides*, that is, in such a way that $|m\rangle$ is thermally lower by 50 cm^{-1} than $|d\rangle$ in *Rb. sphaeroides*, although still higher than $|d\rangle$ by 150 cm^{-1} in *Rps. viridis*. Together with $\Delta G_m - \Delta G_a = 450$ cm^{-1} that we set above, ΔG_a turns out to be set at −500 cm^{-1} for *Rb. sphaeroides* and −300 cm^{-1} for *Rps. viridis*.

States $|m\rangle$ and $|a\rangle$ are connected to each other by the matrix element, J_{am}, for electron transfer between P*•B and P^+•B^-. Adopted from its theoretical calculation, J_{am} was set at 24 cm^{-1} for *Rb. sphaeroides* and 36 cm^{-1} for *Rps. viridis* in the calculation in ref 20b, successfully reproducing the observed data on the initial charge separation in the RC. Therefore, it is set as such also in the present work. Remaining to be set for calculation of $k_{a,d}$ is the matrix element, J_{md}, for excitation transfer between LH1*•P and LH1•P*. Its value was determined for $k_{a,d}$ so as to reproduce its observed value at room temperature. At this step, therefore, the present work has introduced practically only a single adjustable parameter. Direct electronic coupling between $|a\rangle$ of LH1•P^+•B^- and $|d\rangle$ of LH1*•P•B does not exist.

It will be clarified in section III that at room temperature trapping of the excitation energy of the core antenna by the RC proceeds in the ordinary sequential mechnism in both *Rb. sphaeroides* and *Rps. viridis*. In this case, the rate constant for the excitation-energy trapping is given by $k_{a,d}^{(OS)}$ of eq 2.15. Therein, the rate constant $k_{a,m}$ for charge separation from P* to P^+B^-, with magnitudes of $(\sim 3\ ps)^{-1}$,[28] is much larger than the rate constant $k_{m,d}$ for excitation-energy transfer from LH1* to P*, with magnitudes of $(\sim 50\ ps)^{-1}$,[11−18] and the equilirium constant K_m of eq 2.16 is larger than unity. In this situation, $k_{a,d}^{(OS)}$ nearly equals $k_{m,d}$ in eq 2.15. Because $k_{m,d}$ is proportional to J_{md}^2, as explicitly shown in eq D.10 in Appendix D, the detemination of J_{md} mentioned above can be done with a sufficient accuracy. The value of J_{md} thus determined is 4.3 cm^{-1} for *Rb. sphaeroides* and 5.5 cm^{-1} for *Rps. viridis*.

It is worthwhile to mention a significance of such magnitudes of J_{md}. A quite different value of it has been argued,[10] considering that pigments in LH1 are arranged with a rotational symmetry, enclosing the RC on the basis of structure determination of LH1s reconstituted from detergent-solubilized protein complexes.[6,7] In this case, the lowest excited state LH1* of LH1, which constitutes the donor state $|d\rangle$ in the present investigation, is optically forbidden, transforming totally symmetrically on rotation.[29] The excited state P* of the special pair in the RC, which constitutes the intermediate state $|m\rangle$, transforms as a vector on rotation because it is optically allowed with a nonvanishing total transition dipole located at the center of rotation. Electronic states with different rotational symmetries do not interact directly. Accordingly, the matrix element J_{md} for direct electronic interaction between $|d\rangle$ and $|m\rangle$ must vanish in this case. Because the second-lowest doubly degenerate excited states of LH1 are optically allowed,[29] they directly interact with the optically allowed excited-state P* of P, but they are at $\sim$120 cm^{-1} above the lowest excited-state LH1*.[21b] Accordingly, the requirement of $J_{md} = 4.3$ or 5.5 cm^{-1} is not compatible with such a complete-ring structure of LH1.

These values of J_{md} are not in conflict with a recent observation by electron microscopy[8] that LH1 enclosing the RC in the intact membrane has a C-shaped open structure with a cut of about one-fourth of the whole ring under certain conditions. This is because the lowest excited state LH1* of LH1 cannot have the totally symmetric rotational symmetry in a situation in which rotations are no longer symmetry operations. In this case, moreover, the distance for excitation transfer between LH1* and P* is not much larger than their physical sizes, and hence, J_{md} must be calculated with their physical sizes correctly taken into account on the basis of a recent formulation.[30,31] It can be shown by such a calculation that values of J_{md} adopted in the present work are quite reasonable from the standpoint of the C-shaped open structure of LH1.[32] Similar values of J_{md} can be obtained also in a case that LH1* is localized on a restricted number of pigments in LH1 because of interaction with static disorder and phonons even if LH1 has a complete-ring structure.[32]

IV. Numerical Calculation of the Rate Constant $k_{a,d}$

In the excitation-energy trapping in which the initial, the intermediate, and the final states, $|d\rangle$, $|m\rangle$, and $|a\rangle$ of eq 2.1, participate, values of thermal-activation energies for transitions

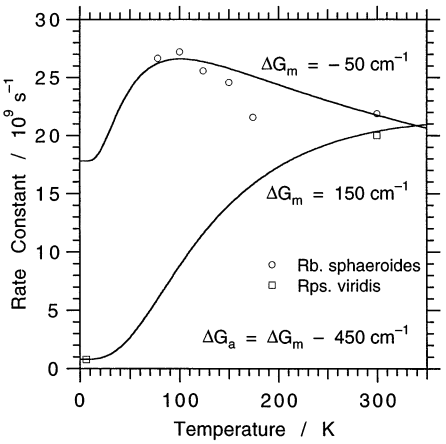

Figure 1. Temperature dependence of the rate constant $k_{a,d}$ for excitation-energy trapping from LH1* by the RC into the charge-separated state $P^+ \cdot B^-$ therein. The solid curves represent the calculated results shown in comparison with the observed data (○ for *Rb. sphaeroides*[15,17a] and □ for *Rps. viridis*[13b,16]).

among them give useful information. For transitions from $|d\rangle$ to $|m\rangle$, $|m\rangle$ to $|a\rangle$, and $|d\rangle$ directly to $|a\rangle$, they are given by $\Delta G^*_{m,d}$ of eq 2.2, $\Delta G^*_{a,m}$ of eq 2.3, and $\Delta G^*_{a,d}$ of eq 2.4, respectively. Parameter setting in section III gives

$$\Delta G^*_{m,d} = 40\ \text{cm}^{-1},\quad \Delta G^*_{a,m} \approx 9\ \text{cm}^{-1},\quad \text{and}$$
$$\Delta G^*_{a,d} \approx 21\ \text{cm}^{-1}\quad \text{for}\quad \textit{Rb. sphaeroides},\quad \text{and}$$
$$\Delta G^*_{m,d} = 160\ \text{cm}^{-1},\quad \Delta G^*_{a,m} \approx 9\ \text{cm}^{-1},\quad \text{and}$$
$$\Delta G^*_{a,d} \approx 68\ \text{cm}^{-1}\quad \text{for}\quad \textit{Rps. viridis}\quad (4.1)$$

Figure 1 shows the temperature dependence of the rate constant $k_{a,d}$ for formation of $|a\rangle$ from $|d\rangle$ mediated by $|m\rangle$, calculated by eq 2.12 with the parameters set in section III. The curves for $\Delta G_m = -50$ and 150 cm^{-1} are for *Rb. sphaeroides* and *Rps. viridis*, respectively. Shown by ○ and □ are the observed data, mentioned in section I, for *Rb. sphaeroides* and *Rps. viridis*, respectively. The matrix element J_{md} for excitation-energy transfer between $|d\rangle$ and $|m\rangle$ is the single adjustable parameter, determined so as to reproduce the observed data of $k_{a,d}$ at room temperature. The value of J_{md} thus determined turned out to be reasonable, as mentioned in section III. We see in Figure 1 that such determination of J_{md} at room temperature lets $k_{a,d}$ simultaneously reproduce the observed data at low temperatures for both species.

Figure 2 shows an analysis of the theoretical curve of $k_{a,d}$ represented by the solid curve, which reproduced the observed data for *Rps. viridis* in Figure 1. The dashed curve therein represents the temperature dependence of $k^{(OS)}_{a,d}$ of eq 2.15, which was obtained by assuming the ordinary sequential mechanism in which the charge separation from $|d\rangle$ to $|a\rangle$ is really mediated at $|m\rangle$ and moreover the transition from $|m\rangle$ to $|a\rangle$ takes place after thermalization of phonons at $|m\rangle$. The dotted curve, on the other hand, represents $k^{(SX)}_{a,d}$, mentioned in section II, which was obtained by assuming the superexchange mechanism in which the transition from $|d\rangle$ to $|a\rangle$ is virtually mediated at $|m\rangle$ before dephasing and thermalization of phonons at $|m\rangle$. The dash−dot curve therein represents the degree of ordinary sequentiality, D_{OS} of eq 2.17.

Above ∼100 K, the solid curve of $k_{a,d}$ in Figure 2 nearly equals the dashed curve of $k^{(OS)}_{a,d}$, while $k_{a,d}$ nearly equals the dotted curve of $k^{(SX)}_{a,d}$ below ∼50 K. Accordingly, the charge separation from $|d\rangle$ to $|a\rangle$ in *Rps. viridis* takes place by the

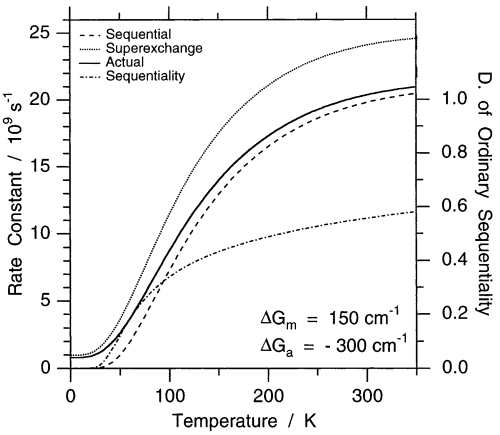

Figure 2. Analysis of the calculation of the rate constant $k_{a,d}$ for excitation-energy trapping from LH1* by the RC in *Rps. viridis*. The solid curve is the same as $k_{a,d}$ reproducing the observed data for *Rps. viridis* in Figure 1. The dashed and the dotted curves represent the rate constants $k^{(OS)}_{a,d}$ and $k^{(SX)}_{a,d}$ in the ordinary sequential and the superexchange mechanisms, respectively, calculated with the same set of parameters as those that gave the $k_{a,d}$. The dash−dot curve represents the degree of ordinary sequentiality, D_{OS}.

ordinary sequential mechanism above ∼100 K while by the superexchange mechanism below ∼50 K. Reflecting this change, the degree of ordinary sequentiality D_{OS} represented by the dash−dot curve has a magnitude of ∼0.3 at ∼75 K, becoming much smaller than unity at lower temperatures while much larger than ∼0.1 at higher temperatures. At 6 K, especially, the observed data of $k_{a,d} = \sim(1.3\ \text{ns})^{-1}$ in *Rps. viridis*, naturally reproduced in Figure 1, are ascribed to the superexchange mechanism, in contrast to those of $k_{a,d} = \sim(50\ \text{ps})^{-1}$ at room-temperature ascribed to the ordinary sequential mechanism. Thus, the serious difficulty in understanding the observed data at 6 K in terms of the ordinary sequential mechanism, mentioned in section I, was reasonably resolved.

At 6 K, the thermal activation energy, $\Delta G^*_{a,d} \approx 68\ \text{cm}^{-1}$ in *Rps. viridis*, for a transition to $|a\rangle$ unistep from $|d\rangle$ is much larger than the thermal energy k_BT (∼4 cm^{-1}). In this situation, the transition should take place by means of quantum-mechanical tunneling of phonons between different configurations of reorganization in association with that of electrons to $LH1 \cdot P^+ \cdot B^-$ unistep from $LH1^* \cdot P \cdot B$.[22] In this regime, $k_{a,d}$ becomes nearly independent of temperature,[22] as in fact seen below ∼25 K in Figure 2.

Shown in Figure 3 is the similar analysis of the theoretical curve of $k_{a,d}$ represented by the solid curve, which reproduced the observed data for *Rb. sphaeroides* in Figure 1. The dashed, the dotted, and the dash−dot curves therein represent the temperature dependence of $k^{(OS)}_{a,d}$, $k^{(SX)}_{a,d}$, and D_{OS}, respectively, calculated with the same set of parameters as those that gave the $k_{a,d}$. At all temperatures in Figure 3, $k_{a,d}$ is nearly equal to $k^{(OS)}_{a,d}$, deviating considerably from $k^{(SX)}_{a,d}$. At all temperatures, therefore, the excitation-energy trapping by the RC in *Rb. sphaeroides* proceeds by the ordinary sequential mechanism. Reflecting this situation, $D_{OS} \gg 0.1$ is realized at all temperatures.

In the ordinary sequential mechanism, the rate constant $k_{a,d}$ is controlled by the transition to $|m\rangle$ from $|d\rangle$ because the subsequent transition to $|a\rangle$ from $|m\rangle$ takes place much more rapidly in the present case as mentioned in sections I and III. The thermal-activation energy $\Delta G^*_{m,d}$ for the first transition is only 40 cm^{-1} in *Rb. sphaeroides*, as shown in eq 4.1. The theoretical expression of the rate constant can be divided into

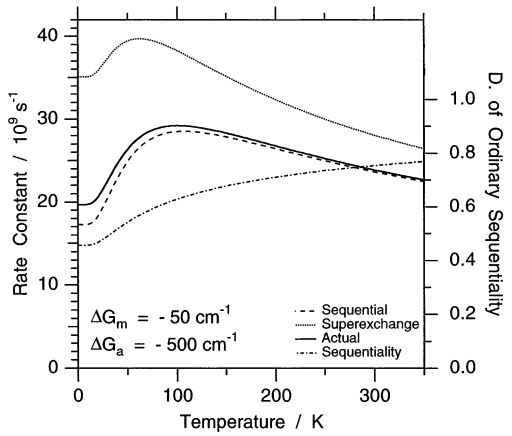

Figure 3. Analysis of the calculation of the rate constant $k_{a,d}$ for excitation-energy trapping from LH1* by the RC in *Rb. sphaeroides*. The solid curve is the same as $k_{a,d}$ reproducing the observed data for *Rb. sphaeroides* in Figure 1. The dashed and the dotted curves represent the rate constants $k_{a,d}^{(OS)}$ and $k_{a,d}^{(SX)}$ in the ordinary sequential and the superexchange mechanisms, respectively, calculated with the same set of parameters as those that gave the $k_{a,d}$. The dash−dot curve represents the degree of ordinary sequentiality, D_{OS}.

the exponential and the preexponential factors. The former carries the thermally activated temperature dependence, while the latter weakly decreases with increasing temperature.[22] When the thermal activation energy is small, such a weak and athermal temperature dependence of the preexponential factor manifests itself in the temperature dependence of the rate constant. This is the reason that $k_{a,d}$ for *Rb. sphaeroides* in Figure 3 weakly increases as the temperature is lowered from room temperature, confirming the consideration in section I explained in more detail in Appendix A. Figure 3 shows that such a temperature dependence is maintained until down to ∼100 K where $k_BT \approx$ 70 cm^{-1}, in agreement with the observed data shown in Figure 1.

Below ∼100 K, $k_{a,d}$ for *Rb. sphaeroides* in Figure 3 begins to decrease. This is because the exponential factor with the thermal-activation energy of 40 cm^{-1} begins to dominate the weak and athermal temperature dependence of the preexponential factor in the $k_{a,d}$ there. No data of the rate constant has been reported in this temperature region for *Rb. sphaeroides*, as seen in Figure 1. Therefore, the temperature dependence of $k_{a,d}$ in this temperature region shown in Figures 1 and 3 for *Rb. sphaeroides* might be included into predictions of the present work. This is, however, a subtle problem because the temperature of ∼100 K varies significantly with a small change in the value of $\Delta G^*_{m,d}$. It is possible that $\Delta G^*_{m,d}$ of eq 2.2 becomes a little smalller by small changes in the parameters therein. In this case, the rate constant $k_{a,d}$ for *Rb. sphaeroides* will still continue to increase with a decrease in temperature until below ∼100 K, as in fact was observed in the rate constant for the initial charge separation from P* in the RC.[28]

The value of $k_{a,d}$ for *Rb. sphaeroides* in Figure 3 becomes nearly independent of temperature below ∼15 K. This reflects the phonon-tunneling regime pointed out for *Rps. viridis* previously in this section. In *Rb. sphaeroides*, however, phonon tunneling is associated with tunneling transfer of excitation only to |m⟩ of LH1·P*·B from |d⟩ of LH1*·P·B in the ordinary sequential mechanism, taking place through the barrier of the thermal-activation energy $\Delta G^*_{m,d} \approx 40$ cm^{-1}.

It has been argued that physical parameters involved in the initial charge separation in the RC change with temperature because of thermal expansion of the protein medium.[33] If these parameters and those involved in the excitation-energy transfer from LH1* to P* were known as a function of temperature, we should use them in the analytic formula shown in Appendix D to calculate the rate constant $k_{a,d}$. At present, however, it is not the case. At present, therefore, let us be content with the temperature-independent parameter setting done in section III, considering that it at least reproduces well the observed temperature dependence, as well as the magnitude of the observed rate constant, as shown in Figure 1.

V. Artificial Modification of the Energy of P* in *Rb. Sphaeroides*

When the transition from |d⟩ to |a⟩ is mediated by |m⟩, the free energy ΔG_m at |m⟩ relative to |d⟩ plays very important roles in the mechanism of the transition.[20b] The value of ΔG_m is about −50 cm^{-1} in *Rb. sphaeroides*, while it is about 150 cm^{-1} in *Rps. viridis*. Accordingly, we expect that the mediation at |m⟩ would be more difficult in *Rps. viridis* than that in *Rb. sphaeroides*. In reality, however, the observed value of the rate constant $k_{a,d}$ is nearly uniform at about $(50\ ps)^{-1}$ at room temperature, as shown in Figure 1. In both species, the mediation at |m⟩ takes place by the ordinary sequential mechanism at room temperature, as shown in Figures 2 and 3. The difference in ΔG_m has been blurred out by thermal activation at room temperature where k_BT amounts to about 210 cm^{-1}. Besides the thermal energy, the sufficiently broad absorption peak of P at room temperature is effective in this result. In fact, its half-width at half-maximum, given by $(2\ \ln\ 2)^{1/2}D_m^{(d)}$, amounts to ∼380 cm^{-1}, becoming comparable even to the excitation-energy difference ΔE (∼350−400 cm^{-1}) between LH1* and P* in *Rps. viridis*. Accordingly, the uphill excitation-energy transfer from LH1* to P* has not been subject to natural selection in the evolution of life at room temperature. However, although physiologically irrelevant, at low temperatures ΔG_m as high as 150 cm^{-1} in *Rps. viridis* cannot be overcome by thermal activation. Correspondingly, the uphill ΔG_m is passed by quantum-mechanical virtual mediation at |m⟩ at low temperatures, as shown in Figure 2. In this case, the rate constant $k_{a,d}$ becomes small, as seen in Figure 1, but still to an astronomical extent larger than the value expected from the ordinary sequential mechanism, as pointed out in section I.

From the comparative analysis between *Rb. sphaeroides* and *Rps. viridis* in section IV, we can expect the following for *Rb. sphaeroides* in which trapping of the excitation energy of LH1* by the RC proceeds by the ordinary sequential mechanism at all temperatures. When ΔG_m is artificially raised from its original value of −50 cm^{-1}, excitation-energy trapping by the RC will shift from the ordinary sequential mechanism in the wild system to the superexchange mechanism also in *Rb. sphaeroides*. This change will occur initially at low temperatures but at higher temperatures as ΔG_m is further raised.

To check such an expectation, ΔG_m was artificially raised initially to 500 cm^{-1} with other parameters unchanged from the values for reproducing $k_{a,d}$ in *Rb. sphaeroides* in Figure 3. The thermal-activation energies in eq 4.1 change to

$$\Delta G^*_{m,d} \approx 560\ cm^{-1}, \quad \Delta G^*_{a,m} \approx 67\ cm^{-1}, \quad \text{and} \quad \Delta G^*_{a,d} \approx 21\ cm^{-1} \quad (5.1)$$

The temperature dependence of $k_{a,d}$ thus obtained is shown by the solid curve in Figure 4 with the dashed, the dotted, and the dash−dot curves therein representing the temperature dependence of $k_{a,d}^{(OS)}$, $k_{a,d}^{(SX)}$, and D_{OS}, respectively. The value of $k_{a,d}$ becomes nearly equal to $k_{a,d}^{(SX)}$ below ∼60 K, ascribed to the

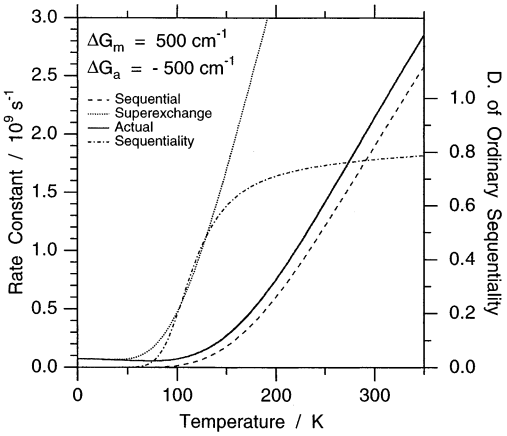

Figure 4. The solid curve represents the rate constant $k_{a,d}$ for excitation-energy trapping from LH1* by the RC in *Rb. sphaeroides* where ΔG_m was artificially changed to 500 cm^{-1} from its wild-type value of -50 cm^{-1}. The dashed and the dotted curves represent the rate constants $k_{a,d}^{(OS)}$ and $k_{a,d}^{(SX)}$ in the ordinary sequential and the superexchange mechanisms, respectively, calculated with the same set of parameters as those that gave the $k_{a,d}$. The dash−dot curve represents the degree of ordinary sequentiality, D_{OS}.

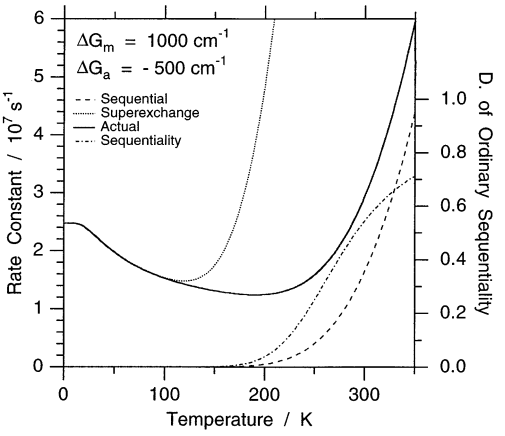

Figure 5. The solid curve represents the rate constant $k_{a,d}$ for excitation-energy trapping from LH1* by the RC in *Rb. sphaeroides* where ΔG_m was artificially changed to 1000 cm^{-1} from its wild-type value of -50 cm^{-1}. The dashed and the dotted curves represent the rate constants $k_{a,d}^{(OS)}$ and $k_{a,d}^{(SX)}$ in the ordinary sequential and the superexchange mechanisms, respectively, calculated with the same set of parameters as those that gave the $k_{a,d}$. The dash−dot curve represents the degree of ordinary sequentiality, D_{OS}.

superexchange mechanism, although it is nearly equal to $k_{a,d}^{(OS)}$ above ∼150 K, ascribed to the ordinary sequential mechanism. Reflecting this change in the character of the energy trapping by the RC, D_{OS} becomes much smaller than unity below ∼60 K, while much larger than 0.1 above ∼150 K. The value of $k_{a,d}$ rises steeply with temperature above ∼125 K. This temperature dependence arises from thermal activation in the initial excitation-energy transfer from LH1* to P* in the ordinary sequential mechanism. In fact, the thermal activation energy of this process is as high as ∼560 cm^{-1} as shown in eq 5.1, becoming considerably larger than the thermal energy.

Subsequently, only ΔG_m was further raised to 1000 cm^{-1} from its original value of -50 cm^{-1} in *Rb. sphaeroides*. The thermal-activation energies in eq 4.1 change to

$$\Delta G^*_{m,d} \approx 1560\ cm^{-1}, \quad \Delta G^*_{a,m} \approx 340\ cm^{-1}, \quad \text{and}$$
$$\Delta G^*_{a,d} \approx 21\ cm^{-1} \quad (5.2)$$

The temperature dependence of $k_{a,d}$ thus obtained is shown by the solid curve in Figure 5 with the dashed, the dotted, and the dash−dot curves therein representing the temperature dependence of $k_{a,d}^{(OS)}$, $k_{a,d}^{(SX)}$, and D_{OS}, respectively. Here, $k_{a,d}$ becomes nearly equal to the dotted curve of $k_{a,d}^{(SX)}$ below ∼150 K, while it is nearly equal to the dashed curve of $k_{a,d}^{(OS)}$ only above room temperature. Accordingly, the ordinary sequential mechanism becomes unrealized in the whole temperature range below about room temperature. This reflects that the intermediate state $|m\rangle$ is too high to be accessible by the aid of thermal activation, as understood from the value of $\Delta G^*_{m,d}$ as high as 1560 cm^{-1} in eq 5.2. In the superexchange mediation realized below ∼150 K, $|m\rangle$ is not really populated but is virtually passed in the transition to the charge-separated state of $|a\rangle$ unistep from LH1*. The thermal activation energy $\Delta G^*_{a,d}$ of this unistep transition is only ∼21 cm^{-1}, as shown in eq 5.2. As pointed out in section IV and also in Appendix A in more detail, when the thermal activation energy is that small, the weak and athermal temperature dependence of the preexponential factor in the expression of the rate constant dominates its temperature dependence. This is the reason that $k_{a,d}$ in Figure 5 weakly decreases with increasing temperature below ∼150 K as soon as $k_{a,d}$ becomes controlled by the superexchange mechanism.

Below about 20 K in Figure 5, $k_{a,d}$ becomes nearly independent of temperature. In this region, the unistep transition in the superexchange mechanism enters the regime of quantum-mechanical tunneling of phonons associated with that of electrons from LH1*•P•B directly to LH1•P^+•B^-.[22] The phonon tunneling takes place to overcome a potential barrier that arises from the reorganization of the medium associated with the electron tunneling, when the barrier is much higher than k_BT.[22] The same regime has already been noted in both *Rb. sphaeroides* and *Rps. viridis* of the wild type in section IV.

VI. Summary

In bacterial photosynthesis, excitation-energy trapping from the excited state of the core antenna LH1 into the initial charge-separated state in the RC is mediated by the excited state of the special pair P of bacteriochlorophylls in the RC. Energy transfer from the lowest excited-state LH1* of LH1 to that P* of P is uphill with the excitation-energy difference between them, ΔE, amounting to about 200 and 350−400 cm^{-1} in *Rb. sphaeroides* and *Rps. viridis*, respectively. Nevertheless, the observed values of the rate constant for the excitation-energy trapping at room temperature are nearly uniform at about (50 ps)$^{-1}$ in both species. It is easily expected that the energy trapping by such uphill excitation-energy transfer will become difficult as the temperature decreases. In *Rb. sphaeroides*, on the contrary, the rate constant slightly increases to (35−45 ps)$^{-1}$ at 77−177 K. In *Rps. viridis*, it does decrease but has still a magnitude as large as (1.3 ns)$^{-1}$ at 6 K. This value deviates to an astronomical extent from the expectation from the ordinary sequential mechanism, in which the initial charge separation starting from P* takes place with thermalization of phonons around P* after an excitation transfer from LH1* to P*.

The present work was devoted to calculating the rate constant for such excitation-energy trapping in purple bacteria. It employed the analytic formula of the rate constant for electron-transfer mediated by a midway molecule in ref 20 by Sumi and Kakitani,[20] with some modifications appropriate for the present problem. The calculation successfully reproduced observed data for both *Rb. sphaeroides* and *Rps. viridis* with respect to both the magnitude and the temperature dependence of the rate constant.

Analysis of the calculation enabled us to obtain the following features. (1) At room temperature, the excitation-energy trapping takes place by the ordinary sequential mechanism in both species. The difference in ΔE between them is blurred out by thermal activation at room temperature. Especially, the half-width at half-maximum of the absorption peak of P*, amounting to about 380 cm^{-1} at room temperature, is effective there, becoming comparable to ΔE even in *Rps. viridis*. (2) In *Rb. sphaeroides*, the ordinary sequential mechanism is maintained at all temperatures. In *Rps. viridis*, on the other hand, this mechanism is maintained only above ~100 K, and it is changed below ~50 K to the superexchange mechanism, where the initial charge separation in the RC takes place unistep from LH1* by quantum-mechanical virtual mediation of P* without real excitation of P. Such a difference in the mechanism of the excitation-energy trapping arises from the difference in the free energy ΔG_m of P* relative to LH1* between them. The value of ΔG_m deviates from ΔE because of reorganizing relaxation of the surrounding medium in association with electronic excitation or deexcitation of pigments. In fact, P* is thermally lower than LH1* by about 50 cm^{-1} in *Rb. sphaeroides*, while P* is thermally still higher than LH1* by about 150 cm^{-1} in *Rps. viridis*. It is also due to this difference that in *Rb. sphaeroides* with $\Delta G_m \approx -50$ cm^{-1}, the rate constant slightly increases with a decrease in temperature until down to ~100 K, controlled by its preexponential factor with such a weak and athermal temperature dependence (noted in Appendix A in more detail). In *Rps. viridis* with $\Delta G_m \approx 150$ cm^{-1}, the superexchange mechanism at 6 K resolves the serious deviation of the observed rate constant from the expectation from the ordinary sequential mechanism.

The matrix element J_{md} for excitation-energy transfer between LH1* and P* is the single adjustable parameter in the parameter setting in section III. It was determined so as to reproduce the observed rate constant at room temperature, at which excitation-energy trapping by the RC proceeds by the ordinary sequential mechanism in both *Rb. sphaeroides* and *Rps. viridis*. Such setting of J_{md} at room temperature lets the theoretical value of the rate constant $k_{a,d}$ simultaneously reproduce the observed data at low temperatures in both species. Especially, this is so also in *Rps. viridis* in which the excitation-energy trapping changes so as to proceed by the superexchange mechanism below ~50 K. This fact could be regarded as one of triumphs of the theory, developed in ref 20, which unifies the ordinary sequential and the superexchnage processes by a single process with the rate constant $k_{a,d}$, called an electronic transition from $|d\rangle$ to $|a\rangle$ mediated by $|m\rangle$ at a midway molecule in general cases.

The value of J_{md} thus determined (4.3 cm^{-1} for *Rb. sphaeroides* and 5.5 cm^{-1} for *Rps. viridis*) is not compatible with a complete-ring structure[6,7] of LH1, which was obtained in structure determination of LH1s reconstituted from detergent-solubilized protein complexes. In such a structure, the lowest excited state LH1* of LH1 is optically forbidden, and the matrix element J_{md} for excitation-energy transfer between LH1* and P* must vanish. The present values of J_{md} are not in conflict with a C-shaped open structure[8] of LH1, which was recently observed by electron microscopy in the intact membrane. In such a C-shaped structure, the lowest excited state LH1* of LH1 becomes optically allowed because rotations are no longer symmetry operations. In this case, moreover, the distance for excitation transfer between LH1* and P* is not much larger than their physical sizes, and hence, J_{md} must be calculated with their physical sizes correctly taken into account on the basis of a recent formulation.[30,31] It can be shown by such a calculation that values of J_{md} adopted in the present work are quite reasonable from the standpoint of the C-shaped open structure of LH1.[32] Similar values of J_{md} can be obtained also in a case that LH1* is localized on a restricted number of pigments in LH1 because of interaction with static disorder and phonons even if LH1 has a complete-ring structure.[32]

In the excitation-energy trapping by charge separation in the RC mediated by P*, the value of ΔG_m plays very important roles in its mechanism. Let us imagine that ΔG_m is artificially raised from its original value of -50 cm^{-1} in *Rb. sphaeroides* with other quantities unchanged. The present work predicts that the excitation-energy trapping by the RC will shift from the ordinary sequential mechanism in the wild system to the superexchange mechanism also in *Rb. sphaeroides*. This change will occur initially at low temperatures, but at higher temperatures as ΔG_m is further raised. As a concrete example, when ΔG_m is slighly raised to 500 cm^{-1}, the ordinary sequential mechanism will be maintained only above ~150 K, and it will be changed to the superexchange mechanism below ~60 K with the temperature dependence of the rate constant shown in Figure 4. When ΔG_m is further raised to 1000 cm^{-1}, the superexchange mechanism will extend to temperatures below ~150 K, but the ordinary sequential mechanism will not be realized below room temperature with the temperature dependence of the rate constant shown in Figure 5.

Acknowledgment. The author thanks Professor S. Itoh of Nagoya University for informing him of experimental features about uphill excitation-energy transfer from the core antenna to P in the RC in the primary process of photosynthesis.

Appendix A: Rate Constant of a Single-Step Electronic Transition

When a single-step electronic transition is endothermic with a rate constant k_+, its reverse reaction is exothermic with a rate constant k_-. They are related to each other by the law of chemical equilibrium as $k_+ = k_- \exp(-|\Delta G|/(k_B T))$, where $|\Delta G|$ represents the difference in the free energy before and after the electronic transition, being taken as positive. When the thermal activation energy of k_- is written as ΔG^* (≥ 0), this relation tells us that the thermal activation energy of k_+ is given by $\Delta G^* + |\Delta G|$. It is larger than $|\Delta G|$, as mentioned in section I of the text.

When a reaction is exothermic or only weakly endothermic with $|\Delta G| \ll k_B T$, its rate constant k is exactly or nearly equal to k_-, respectively. In such cases, simultaneously when also the thermal activation energy, ΔG^* (≥ 0), of k_- is much smaller than $k_B T$, the rate constant k can be approximated by the preexponential factor of k_-, which equals that of k. The preexponential factor weakly decreases with temperature.[22] Therefore, only when a reaction is either exothermic or only weakly endothermic with $|\Delta G| \ll k_B T$, its rate constant k can have a temperature dependence weakly decreasing with it, as mentioned in section I of the text.

The ratio of k_+ between temperatures T_1 and T_2 is given by $k_+(T_1)/k_+(T_2) = [k_-(T_1)/k_-(T_2)] \exp[(T_2^{-1} - T_1^{-1})|\Delta G|/k_B]$. When $T_1 < T_2$, the first factor $k_-(T_1)/k_-(T_2)$ therein is much smaller than unity when $\Delta G^* \gg k_B T_1$ or nearly equal to unity when $\Delta G^* \lesssim k_B T_1$ because in the latter case both $k_-(T_1)$ and $k_-(T_2)$ become nearly equal to their preexponential factors with only a weak temperature dependence. Therefore, for the values of a rate constant k of an endothermic reaction at temperatures T_1 and T_2, we get a relation used in section I of the text as

$$k(T_1)/k(T_2) \lesssim \exp[(T_2^{-1} - T_1^{-1})|\Delta G|/k_B] \quad \text{when} \quad T_1 < T_2 \tag{A.1}$$

Appendix B: Reorganization Energy

In correspondence with whether the electron system is at the state of $|d\rangle$, $|m\rangle$, or $|a\rangle$, the phonon system is described by the Hamiltonian H_d, H_m, or H_a, respectively. The phonon system at $|m\rangle$ is taken as the reference frame in describing phonons at $|d\rangle$ or $|a\rangle$, as mentioned in section II. In this frame, it is convenient to express H_m as

$$H_m = \frac{1}{2}\sum_{\ell}\hbar\omega_{\ell}(p_{\ell}^2 + q_{\ell}^2) + \Delta G_m \qquad (B.1)$$

where ΔG_m represents the free energy at $|m\rangle$ relative to $|d\rangle$, and q_{ℓ} and p_{ℓ} represent, respectively, the coordinate and its conjugate momentum operators for the ℓth normal mode of phonons with angular frequency ω_{ℓ}, taken so as to satisfy

$$[p_{\ell},q_{\ell'}] \,(\equiv p_{\ell}q_{\ell'} - q_{\ell'}p_{\ell}) = -i\delta_{\ell,\ell'} \qquad (B.2)$$

At $|d\rangle$, LH1 is electronically excited but P is not, while at $|m\rangle$, LH1 is not excited but P is. Therefore, H_d reflects not only reorganization of the medium around LH1 in association with its excitation, but also that around P in association with its deexcitation. Following the formulation in ref 20, let us assume that phonon modes participating in the former do not participate in the latter, and vice versa, because LH1 and P are apart in space by several dozens of angstroms.[4−6] Phonons around LH1 and P are discriminated by suffixes *i* and *j*, respectively. Let us write, accordingly, that the coordinate of the *i*th phonon mode shifts by $\sqrt{2}\chi_i$ in association with excitation of LH1 and that of the *j*th mode shifts by $\sqrt{2}\xi_j$ in association with deexcitation of P. Phonons around B are discriminated by suffixes *k*. Under the assumption that these modes do not participate in the reorganization by phonon modes with suffixes *i* and *j* around LH1 and P, respectively, coordinates of phonon modes with suffixes *k* do not shift in association with excitation transfer between $|d\rangle$ and $|m\rangle$. Reflecting these situations, H_d emerges as

$$H_d = \frac{1}{2}\sum_i \hbar\omega_i[p_i^2 + (q_i - \sqrt{2}\chi_i)^2] + \frac{1}{2}\sum_j \hbar\omega_j[p_j^2 + (q_j - \sqrt{2}\xi_j)^2] + \frac{1}{2}\sum_k \hbar\omega_k(p_k^2 + q_k^2) \qquad (B.3)$$

In section II, the energies of reorganization of the medium in association with electronic excitation of LH1 and P were expressed as λ_d and $\lambda_m^{(d)}$, respectively. We get from eq B.3

$$\lambda_d = \sum_i \hbar\omega_i\chi_i^2 \quad \text{and} \quad \lambda_m^{(d)} = \sum_j \hbar\omega_j\xi_j^2 \qquad (B.4)$$

At $|a\rangle$, P is oxidized into P^+ but B is reduced into B^-, while at $|m\rangle$, P is electronically excited into P* but B is not. Accordingly, H_a reflects not only reorganization of the medium around P in association with its oxidation from P*, but also that around B in association with its reduction. This situation is described in such a way that the coordinate of the *j*th phonon mode around P shifts by $\sqrt{2}\eta_j$ in association with the former and that of the *k*th mode around B shifts by $\sqrt{2}\zeta_k$ in association with the latter. Coordinates of phonon modes with suffixes *i* do not shift in association with electron transfer between $|a\rangle$ and $|m\rangle$. Correspondingly, H_a can be expressed as

$$H_a = \frac{1}{2}\sum_i \hbar\omega_i(p_i^2 + q_i^2) + \frac{1}{2}\sum_j \hbar\omega_j[p_j^2 + (q_j - \sqrt{2}\eta_j)^2] + \frac{1}{2}\sum_k \hbar\omega_k[p_k^2 + (q_k - \sqrt{2}\zeta_k)^2] + \Delta G_a \qquad (B.5)$$

where ΔG_a represents the free energy at $|a\rangle$ relative to $|d\rangle$. In section II, the energy of reorganization of the medium in association with oxidation of P from P* and reduction of B was expressed as $\lambda_m^{(a)}$ and λ_a, respectively. They are given by

$$\lambda_m^{(a)} = \sum_j \hbar\omega_j\eta_j^2 \quad \text{and} \quad \lambda_a = \sum_k \hbar\omega_k\zeta_k^2 \qquad (B.6)$$

In the charge separation to $|a\rangle$ unistep from $|d\rangle$, LH1* is deexcited, P is oxidized into P^+, and B is reduced into B^-. Reorganization of the medium in association with this unistep charge separation is reflected by the difference in phonon configuration between the ground states of Hamiltonians H_d of eq B.3 and H_a of eq B.5. Energies of the reorganization of the medium around LH1 and B are given by λ_d in eq B.4 and λ_a in eq B.6, respectively. That around P is given by the sum of $\hbar\omega_j(\xi_j - \eta_j)^2$ in phonon modes with suffixes *j*, and it is expressed as $\lambda_m^{(a)} + \lambda_m^{(d)} - 2\lambda_m$ by newly introducing

$$\lambda_m = g(\lambda_m^{(a)}\lambda_m^{(d)})^{1/2} \quad \text{with} \quad g \equiv \Big(\sum_j \hbar\omega_j\xi_j\eta_j\Big)\Big/(\lambda_m^{(a)}\lambda_m^{(d)})^{1/2} \qquad (B.7)$$

The total reorganization energy associated with the charge separation to $|a\rangle$ unistep from $|d\rangle$ is given by $\lambda_a + \lambda_m^{(a)} + \lambda_m^{(d)} - 2\lambda_m + \lambda_d$.

The absolute value of *g* defined by eq B.7 is smaller than unity, ensured by Schwarz's inequality. Therefore, $\lambda_m^{(a)} + \lambda_m^{(d)} - 2\lambda_m$ is positive, even if λ_m is positive. Here, $\lambda_m^{(a)}$ in eq B.6 and $\lambda_m^{(d)}$ in eq B.4 represent the energy of reorganization of the medium associated with deexcitation of P* and that associated with oxidation of P*, respectively. Correspondingly, $(\hbar\omega_j/\lambda_m^{(d)})^{1/2}\xi_j$ and $(\hbar\omega_j/\lambda_m^{(a)})^{1/2}\eta_j$ can be regarded as the projection onto the *j*th-mode-coordinate axis of a unit vector in the direction of the reorganizing distortion associated with the former and the latter, respectively, in the multidimensional phonon-coordinate space. Therefore, *g* in eq B.7 represents the direction cosine between the two directions. In general, *g* does not vanish because the two directions are not perpendicular to each other, that is, because phonon modes participating in the reorganization associated with the former overlap with those participating in the reorganization associated with the latter. This occurs because these modes represent vibrations in the same medium around P.

Appendix C: Rate Constant $k_{a,d}$

Let us express by J_{md} the matrix element of electronic-excitation transfer between $|d\rangle$ and $|m\rangle$ and by J_{am} that of electron transfer between $|m\rangle$ and $|a\rangle$. Both of them can be taken as real. As in Appendix B, Hamiltonians for phonons are expressed as H_d, H_m, and H_a when the electronic system is at the state of $|d\rangle$, $|m\rangle$, and $|a\rangle$, respectively. Thermal average over phonon states in H_d is represented by $\langle\cdots\rangle_d$.

The theory of ref 20 is based on the perturbational treatment with respect to J_{md} and J_{am} with its renormalization. As a formal expression,[20a] this theory gives $F(\tau)$ in eq 2.12 for the rate constant $k_{a,d}$ of a transition from $|d\rangle$ to $|a\rangle$ mediated by $|m\rangle$, as

$$F(\tau) = f(\tau)\exp[-\int_0^\tau C_m(t)\,dt] \quad (C.1)$$

with

$$f(\tau) \equiv \left(\frac{J_{am}J_{md}}{\hbar^2}\right)^2 \int\int_{|\mu-\sigma|<2\tau} W(\mu,\sigma;\tau)\,d\mu\,d\sigma \quad (C.2)$$

and

$$W(\mu,\sigma;\tau) \equiv \langle e^{iH_m(\tau+\mu/2-\sigma/2)/\hbar}\, e^{iH_a\sigma/\hbar}\, e^{-iH_m(\tau-\mu/2+\sigma/2)/\hbar}\, e^{-iH_d\mu/\hbar}\rangle_d \quad (C.3)$$

where $f(\tau)$ of eq C.2 is obtained by the second-order expansion with respect to both J_{md} and $J_{am'}$ and the remaining exponential factor in eq C.1 arises from its renormalization. $C_m(t)$ can be approximated by the rate constant for hot decay of the electronic excitation at $|m\rangle$ to $|d\rangle$ and $|a\rangle$ at time t (>0) during thermalization of phonons under the condition that $|m\rangle$ is produced by excitation transfer from $|d\rangle$ at $t = 0$.

As in ref 20b, reorganizing motions of phonons associated with an electronic transition, mentioned in Appendix B, are treated semiclassically. In such a treatment, we are allowed to expand the logarithm of $W(\mu,\sigma;\tau)$ of eq C.3 up to second order in both μ and σ.[22] Moreover, following ref 20 as in Appendix B, we assume that phonon modes with suffixes i participating in the reorganization of the medium around LH1 do not participate in the reorganization of the medium by phonon modes with suffixes j and k around P and B, respectively, in eqs B.3 and B.5, and vice versa, considering that LH1, P, and B are sufficiently apart in space. Applying these treatments, we can manipulate the right-hand side of eq C.3 as explained in ref 20b, reducing it to

$$\ln[W(\mu,\sigma;\tau)] \approx \ln[W(\mu,\sigma;\infty)] - i2\lambda_m(\tau)\sigma/\hbar + D_m(\tau)^2\mu\sigma/\hbar^2 \quad (C.4)$$

with

$$\ln[W(\mu,\sigma;\infty)] \approx i(\lambda_m^{(d)} + \lambda_d + \Delta G_m)\mu/\hbar - {}^1/_2(D_m^{(d)2} + D_d{}^2)\mu^2/\hbar^2 + i(\lambda_m^{(a)} + \lambda_a + \Delta G_a - \Delta G_m)\sigma/\hbar - {}^1/_2(D_m^{(a)2} + D_a{}^2)\sigma^2/\hbar^2 \quad (C.5)$$

$$\lambda_m(\tau) = \sum_j \hbar\omega_j\xi_j\eta_j \cos(\omega_j\tau) \quad (C.6)$$

$$D_m(\tau)^2 = \sum_j (\hbar\omega_j)^2\xi_j\eta_j \coth(\beta\hbar\omega_j/2)\cos(\omega_j\tau) \quad \text{with} \quad \beta \equiv 1/(k_BT) \quad (C.7)$$

$$D_d{}^2 = \sum_i (\hbar\omega_i\chi_i)^2 \coth(\beta\hbar\omega_i/2)$$

$$D_a{}^2 = \sum_k (\hbar\omega_k\chi_k)^2 \coth(\beta\hbar\omega_k/2) \quad (C.8)$$

$$D_m^{(d)2} = \sum_j (\hbar\omega_j\xi_j)^2 \coth(\beta\hbar\omega_j/2)$$

$$D_m^{(a)2} = \sum_j (\hbar\omega_j\eta_j)^2 \coth(\beta\hbar\omega_j/2) \quad (C.9)$$

Equations C.1 to C.3 for calculating the rate constant $k_{a,d}$ are formally the same as those in ref 20b, but therein an equation (B.7 multiplied by both eqs B.5 and B.6 side by side, although $-i$ on the right-hand side of eq B.5 is a mistake for i) corresponding to eq C.5 was

$$\ln[W(\mu,\sigma;\infty)] \approx i(\lambda_m + \lambda_d + \Delta G_m)\mu/\hbar - \frac{1}{2}(D_m{}^2 + D_d{}^2)\mu^2/\hbar^2 + i(\lambda_m + \lambda_a + \Delta G_a - \Delta G_m)\sigma/\hbar - \frac{1}{2}(D_m{}^2 + D_a{}^2)\sigma^2/\hbar^2$$

besides a change in the expression of both $\lambda_m(\tau)$ of eq C.6 and $D_m(\tau)^2$ of eq C.7. Therefore, eq C.5 can be obtained by applying the replacements of eq 2.11 to this $\ln[W(\mu,\sigma;\infty)]$ in ref 20b. It can be shown, similarly, that the replacement concerning $\lambda_d(t)$ in eq 2.11 is used for obtaining $C_m(t)$ of the present problem from that in ref 20b, where

$$\lambda_d(\tau) \equiv \sum_i \hbar\omega_i\chi_i{}^2 \cos(\omega_i\tau) \quad \text{and} \quad \lambda_m^{(d)}(\tau) \equiv \sum_j \hbar\omega_j\xi_j{}^2 \cos(\omega_j\tau) \quad (C.10)$$

We see, thus, that $k_{a,d}$ of the present problem can be obtained by applying the replacements of eq 2.11 to the analytic formula of $k_{a,d}$ for the similar problem in ref 20b.

The average energy quantum of phonons is taken at the same $\hbar\varpi$ commonly among the three groups of phonon modes discriminated by suffixes i, j, and k in eqs C.8 and C.9. $D_d{}^2$, $D_m^{(d)2}$, $D_m^{(a)2}$, and $D_a{}^2$ in eqs C.8 and C.9 approach $2k_BT\lambda_d$, $2k_BT\lambda_m^{(d)}$, $2k_BT\lambda_m^{(a)}$, and $2k_BT\lambda_a$, respectively, when $k_BT \gg \hbar\varpi$, where λ_d, $\lambda_m^{(d)}$, $\lambda_m^{(a)}$, and λ_a are defined by eqs B.4 and B.6. Because the effective temperature T' defined by eq 2.6 approaches T when $k_BT \gg \hbar\varpi$, as in eq 2.6, $D_d{}^2$, $D_m^{(d)2}$, $D_m^{(a)2}$, and $D_a{}^2$ are approximated as eq 2.4, as in ref 20b. When we introduce $D_m{}^2$ as the value of $D_m(t)^2$ at $t = 0$, its relation with λ_m of eq B.7 can be approximated by eq 2.8, similarly to those of $D_d{}^2$, $D_m^{(d)2}$, $D_m^{(a)2}$, and $D_a{}^2$ mentioned above.

Both $\lambda_m(\tau)$ of eq C.6 and $D_m(\tau)^2$ of eq C.7 decay to zero as time τ increases, starting from λ_m of eq B.7 and $D_m{}^2$ defined above, respectively, at $\tau = 0$. The decay (i.e., thermalization) takes place because of dephasing among phonons in the course of reorganization of the medium at $|m\rangle$, as apparent from the expression of $\lambda_m(\tau)$ in eq C.6 and $D_m(\tau)^2$ in eq C.7. The decay time has been called the dephasing-thermalization time of phonons, τ_m, as in section II, and $1/\tau_m$ can be estimated by the average width in frequency dispersion of phonons contributing to the reorganization.[20,23] With this τ_m, the decay of $\lambda_m(\tau)$ and $D_m(\tau)^2$ can be approximated by eq 2.9, as rationalized in ref 20b. Under a simplification that the same value of τ_m is taken for dephasing and thermalization of phonons around LH1, we get approximations in eq 2.10.

Appendix D: Analytic Formula for $k_{a,d}$

When $F(\tau)$ on the right-hand side of eq 2.12 is divided into $F(\tau) = f(\tau)\exp[-\int_0^\tau C_m(t)\,dt]$ as in eq C.1, both $f(\tau)$ and $C_m(t)$ are given as analytic functions shown below in the semiclassical approximation for phonons contributing to the reorganization energies. First, for $f(\tau)$,

$$f(\tau) \approx \left(\frac{J_{am}J_{md}}{\hbar}\right)^2 \frac{2\pi\exp(-S_a)}{[(D_a{}^2 + D_m^{(a)2})(D_m^{(d)2} + D_d{}^2) - D_m(\tau)^4]} \sum_{n=0}^{\infty} \frac{S_a{}^2}{n!}$$

$$\exp\left[-\frac{(n\hbar\omega_a + E_{am}(\tau) + E_{md})^2/2}{D_a{}^2 + D_m^{(a)2} + D_m^{(d)2} + D_a{}^2 - 2D_m(\tau)^2} - y^2\right] \mathcal{R}[\mathrm{erf}(x+iy)] \quad (D.1)$$

with

$$x = \left[2\frac{(D_a{}^2 + D_m^{(a)2})(D_m^{(d)2} + D_d{}^2) - D_m(\tau)^4}{D_a{}^2 + D_m^{(a)2} + D_m^{(d)2} + D_d{}^2 - 2D_m(\tau)^2}\right]^{1/2}\frac{\tau}{\hbar} \quad \text{(D.2)}$$

$$y = \left[|[D_d{}^2 + D_m^{(d)2} - D_m(\tau)^2][n\hbar\omega_a + E_{am}(\tau)] - [D_a{}^2 + D_m^{(a)2} - D_m(\tau)^2]E_{md}|\right]\Big/\left[\{2[(D_a{}^2 + D_m^{(a)2})(D_m^{(d)2} + D_d{}^2) - D_m(\tau)^4][D_a{}^2 + D_m^{(a)2} + D_m^{(d)2} + D_d{}^2 - 2D_m(\tau)^2]\}^{1/2}\right] \quad \text{(D.3)}$$

$$E_{am}(\tau) = \Delta G_a - \Delta G_m + \lambda_a + \lambda_m^{(a)} - 2\lambda_m(\tau) \quad \text{(D.4)}$$

and

$$E_{md} = \Delta G_m + \lambda_m^{(d)} + \lambda_d \quad \text{(D.5)}$$

where $\mathcal{R}[\mathrm{erf}(x + iy)]$ represents taking the real part of the error function of a complex argument $z = x + iy$ defined[34] by $\mathrm{erf}(z) = (2/\sqrt{\pi})\int_0^z \exp(-t^2)\,\mathrm{d}t$.

For $C_m(t)$, when $k_{d,m}(t)$ and $k_{a,m}(t)$ represent the rate constants for hot decay of the electronic excitation at $|m\rangle$ to $|d\rangle$ and $|a\rangle$, respectively, at time t (>0) during thermalization of phonons under the condition that $|m\rangle$ is produced by excitation transfer from $|d\rangle$ at $t = 0$,

$$C_m(t) = k_{d,m}(t) + k_{a,m}(t) \quad \text{(D.6)}$$

with

$$k_{d,m}(t) = \frac{J_{md}{}^2}{\hbar}\left(\frac{2\pi}{D_d{}^2 + D_m^{(d)2}}\right)^{1/2}\exp\left(-\frac{E_{dm}(t)^2}{2(D_d{}^2 + D_m^{(d)2})}\right) \quad \text{(D.7)}$$

$$k_{a,m}(t) = \frac{J_{am}{}^2}{\hbar}\left(\frac{2\pi}{D_a{}^2 + D_m^{(a)2}}\right)^{1/2} e^{-S_a}\sum_{n=0}^{\infty}\frac{S_a{}^n}{n!}\exp\left(-\frac{[n\hbar\omega_a + E_{am}(t)]^2}{2(D_a{}^2 + D_m^{(a)2})}\right) \quad \text{(D.8)}$$

and

$$E_{dm}(t) = \lambda_d + \lambda_m^{(d)} - 2\lambda_d(t) - 2\lambda_m^{(d)}(t) - \Delta G_m \quad \text{(D.9)}$$

To actually calculate $k_{a,d}$ by eq 2.12 with eq C.1 and eqs D.1−D.9, it is convenient to use a method of its approximate calculation shown in eq 5.30 of ref 20b.

When $t \gg \tau_m$, $k_{d,m}(t)$ and $k_{a,m}(t)$ approach the rate constants $k_{d,m}$ and $k_{a,m}$, respectively, for an electronic transition from $|m\rangle$ to $|d\rangle$ and $|a\rangle$ after thermalization of phonons at $|m\rangle$. Therefore, $k_{a,m}$ and $k_{d,m}$ can be obtained by letting $\lambda_d(t)$ and $\lambda_m^{(d)}(t)$ in eq D.9 and $\lambda_m(\tau)$ in eq D.4, respectively, vanish. The rate constant $k_{m,d}$ for an electronic transition from $|d\rangle$ to $|m\rangle$ in the semiclassical approximation for phonons is given by

$$k_{m,d} = \frac{J_{md}{}^2}{\hbar}\left(\frac{2\pi}{D_d{}^2 + D_m^{(d)2}}\right)^{1/2}\exp\left(-\frac{(\Delta G_m + \lambda_d + \lambda_m^{(d)})^2}{2(D_d{}^2 + D_m^{(d)2})}\right) \quad \text{(D.10)}$$

With $k_{a,m}$ and $k_{m,d}$, the rate constant $k_{a,d}^{(OS)}$ in the ordinary sequential mechanism can be obtained by eq 2.15. The degree of ordinary sequentiality D_{OS} of eq 2.17 can be obtained by calculating the survival probability P_m of an electronic excitation at P until time $\bar{\tau}_m$ by

$$P_m = \exp[-\int_0^{\bar{\tau}_m} C_m(t)\,\mathrm{d}t] \quad \text{with} \quad \bar{\tau}_m \approx 1.52\tau_m \quad \text{(D.11)}$$

References and Notes

(1) (a) Fleming, G. R.; van Grondelle, R. *Phys. Today* **1994**, *47*, 48. (b) Hu, X.; Schulten, K. *Phys. Today* **1997**, *50*, 28. (c) Cogdell, R. J.; Lindsay, J. G. *New Phytol.* **2000**, *145*, 167.

(2) (a) Deisenhofer, J.; Epp, O.; Miki, K.; Huber, R.; Michel, H. *J. Mol. Biol.* **1984**, *180*, 385. (b) Allen, J. P.; Feher, G.; Yeates, T. O.; Komiya, H.; Rees, D. C. *Proc. Natl. Acad. Sci. U.S.A.* **1987**, *84*, 5730, 6162. (c) Hoff, A. J.; Deisenhofer, J. *Phys. Rep.* **1997**, *287*, 1.

(3) (a) McDermott, G.; Prince, S. M.; Freer, A. A.; Hawthornthwaite-Lawless, A. M.; Papiz, M. Z.; Cogdell, R. J.; Isaacs, N. W. *Nature* **1995**, *374*, 512. (b) Koepke, J.; Hu, X.; Muenke, C.; Schulten, K.; Michel, H. *Structure* **1996**, *4*, 581.

(4) Germeroth, L.; Lottspeich, F.; Roberts, B.; Michel, H. *Biochemistry* **1993**, *32*, 5615.

(5) McLuskey, K.; Prince, S. M.; Cogdell, R. J.; Isaacs, N. W. *Biochemistry* **2001**, *40*, 8783.

(6) Karrasch, S.; Bullough, P. A.; Ghosh, R. *EMBO J.* **1995**, *14*, 631.

(7) (a) Walz, T.; Ghosh, R. *J. Mol. Biol.* **1997**, *265*, 107. (b) Ikeda-Yamazaki, I.; Odahara, T.; Mitsuoka, K.; Fujiyoshi, Y.; Murata, K. *FEBS Lett.* **1998**, *425*, 505. (c) Stahlberg, H.; Dubochet, J.; Vogel, H.; Ghosh, R. *J. Mol. Biol.* **1998**, *282*, 819. (d) Walz, T.; Jamieson, S. J.; Bowers, C. M.; Bullough, P. A.; Hunter, C. N. *J. Mol. Biol.* **1998**, *282*, 833. (e) Qian, P.; Yagura, T.; Koyama, Y.; Cogdell, R. J. *Plant Cell Physiol.* **2000**, *41*, 1347.

(8) (a) Jungas, C.; Ranck, J.-L.; Rigaud, J.-L.; Joliot, P.; Verméglio, A. *EMBO J.* **1999**, *18*, 534. (b) Francia, F.; Wang, J.; Venturoli, G.; Melandri, B. A.; Barz, W. P.; Oesterhelt, D. *Biochemistry* **1999**, *38*, 6834. (c) Leupold, D.; Voigt, B.; Beeken, W.; Stiel, H. *FEBS Lett.* **2000**, *480*, 73.

(9) (a) Schmidt, S.; Arlt, T.; Hamm, P.; Huber, H.; Nägele, T.; Wachtveitl, J.; Meyer, M.; Scheer, H.; Zinth, W. *Chem. Phys. Lett.* **1994**, *223*, 116. (b) Zinth, W.; Arlt, T.; Wachtveitl, J. *Ber. Bunsen-Ges. Phys. Chem.* **1996**, *100*, 1962. (c) Spörlein, S.; Zinth, W.; Meyer, M.; Scheer, H.; Wachtveitl, J. *Chem. Phys. Lett.* **2000**, *322*, 454.

(10) (a) Hu, X.; Ritz, T.; Damjanović, A.; Schulten, K. *J. Phys. Chem. B* **1997**, *101*, 3854. (b) Hu, X.; Schulten, K. *Biophys. J.* **1998**, *75*, 683. (c) Hu, X.; Damjanović, A.; Ritz, T.; Schulten, K. *Proc. Natl. Acad. Sci. U.S.A.* **1998**, *95*, 5935. (d) Ritz, T.; Park, S.; Schulten, K. *J. Phys. Chem. B* **2001**, *105*, 8259.

(11) As a review: Freiberg, A. In *Anoxygenic Photosynthetic Bacteria*; Blankenship, R. E., Madigan, M. T., Bauer, C. E., Eds.; Kluwer Academic Publishers: Dordrecht, Netherlands, 1995; pp 385−398.

(12) Trissl, H.-W. *Photosynth. Res.* **1993**, *35*, 247.

(13) (a) Holt, A. S.; Clayton, R. K. *Photochem. Photobiol.* **1965**, *4*, 829. (b) Kleinherenbrink, F. A. M.; Deinum, G.; Otte, S. C. M.; Hoff, A. J.; Amesz, J. *Biochim. Biophys. Acta* **1992**, *1099*, 175.

(14) Permentier, H. P.; Neerken, S.; Overmann, J.; Amesz, J. *Biochemistry* **2001**, *40*, 5573.

(15) Beekman, L. M. P.; van Mourik, F.; Jones, M. R.; Visser, M.; Hunter, C. N.; van Grondelle, R. *Biochemistry* **1994**, *33*, 3143.

(16) (a) Kleinherenbrink, F. A. M.; Cheng, P.; Amesz, J.; Blankenship, R. E. *Photochem. Photobiol.* **1993**, *57*, 13. (b) Timpmann, K.; Freiberg, A.; Sundström, V. *Chem. Phys.* **1995**, *194*, 275.

(17) (a) Visscher, K. J.; Bergström, H.; Sundström, V.; Hunter, C. N.; van Grondelle, R. *Photosynth. Res.* **1989**, *22*, 211. (b) Kennis, J. T. M.; Aartsma, T. J.; Amesz, J. *Biochim. Biophys. Acta* **1994**, *1188*, 278. (c) Kramer, H.; Deinum, G.; Gardiner, A. T.; Gogdell, R. J.; Francke, C.; Aartsma, T. J.; Amesz, J. *Biochim. Biophys. Acta* **1995**, *1231*, 33. (d) Freiberg, A.; Allen, J. P.; Williams, J. C.; Woodbury, N. W. *Photosynth. Res.* **1996**, *48*, 309. (e) Chiou, H. C.; Lin. S.; Blankenship, R. E. *J. Phys. Chem. B* **1997**, *101*, 4136. (f) Permentier, H. P.; Neerken, S.; Schmidt, K. A.; Overmann, J.; Amesz, J. *Biochim. Biophys. Acta* **2000**, *1460*, 338.

(18) (a) van Grondelle, R.; Dekker, J. P.; Gillbro, T.; Sundström, V. *Biochim. Biophys. Acta* **1994**, *1187*, 1. (b) Sundström, V.; van Grondelle, R. In *Anoxygenic Photosynthetic Bacteria*; Blankenship, R. E., Madigan, M. T., Bauer, C. E., Eds.; Kluwer Academic Publishers: Dordrecht, Netherlands, 1995; pp 349−372.

(19) Kramers, H. A. *Physica* **1934**, *1*, 182.

(20) (a) Sumi, H.; Kakitani, T. *Chem. Phys. Lett.* **1996**, *252*, 85. (b) Sumi, H.; Kakitani, T. *J. Phys. Chem. B* **2001**, *105*, 9603.

(21) (a) Reddy, N. R. S.; Picorel, R.; Small, G. J. *J. Phys. Chem.* **1992**, *96*, 6458. (b) Wu, H.-M.; Rätsep, M.; Jankowiak, R.; Cogdell, R. J.; Small,

G. J. *J. Phys. Chem. B* **1998**, *102*, 4023. (c) Rätsep, M.; Wu, H.-M.; Hayes, J. M.; Blankenship, R. E.; Cogdell, R. J.; Small, G. J. *J. Phys. Chem. B* **1998**, *102*, 4035.

(22) For example: Sumi, H. In *Electron Transfer in Chemistry*; Balzani, V., Ed.; Wiley-VCH: Weinheim, Germany, 2001; Vol. 1 (Principles, Theories, Techniques and Methods), p 64.

(23) Toyozawa, Y. *J. Phys. Soc. Jpn*. **1976**, *41*, 400. (b) Kotani, A.; Toyozawa, Y. *J. Phys. Soc. Jpn*. **1976**, *41*, 1699. (c) Toyozawa, Y.; Kotani, A.; Sumi, A. *J. Phys. Soc. Jpn*. **1977**, *42*, 1495.

(24) Lyle, P. A.; Kolaczkowski, S. V.; Small, G. L. *J. Phys. Chem*. **1993**, *97*, 6924.

(25) Woodbury, N. W.; Allen, J. P. In *Anoxygenic Photosynthetic Bacteria*; Blankenship, R. E., Madigan, M. T., Bauer, C. E., Eds.; Kluwer Academic Publishers: Dordrecht, Netherlands, 1995; pp 527−557.

(26) Ahn, J. S.; Kanematsu, Y.; Enomoto, M.; Kushida, T. *Chem. Phys. Lett*. **1995**, *215*, 336.

(27) Nakashima, S.; Seike, K.; Nagasawa, Y.; Okada, T.; Sato, M.; Kohzuma, T. *J. Chin. Chem. Soc*. **2000**, *47*, 693; *Chem. Phys. Lett*. **2000**, *331*, 369.

(28) Fleming, G. R.; Martin, J.-L.; Breton, J. *Nature* **1988**, *333*, 190.

(29) (a) Novoderezhkin, V. I.; Razjivin, A. P. *Photosynth. Res*. **1994**, *42*, 9. (b) Damjanović, A.; Ritz, T.; Schulten, K. *Int. J. Quantum Chem*. **2000**, *77*, 139.

(30) Sumi, H. *J. Phys. Chem. B* **1999**, *103*, 252; *J. Lumin*. **2000**, *331*, 396; *Chem. Rec*. **2001**, *1*, 480.

(31) Mukai, K.; Abe, S.; Sumi, H. *J. Phys. Chem. B* **1999**, *103*, 6096; *J. Lumin*. **2000**, *331*, 818.

(32) Mukai, K. Private communication, 2000.

(33) For recent examples, see: Chang, C. H.; Hayashi, M.; Liang, K. K.; Chang, R.; Lin, S. H. *J. Phys. Chem. B* **2001**, *105*, 1216 and references therein.

(34) Abramowitz, M.; Stegun, I. A. *Handbook of Mathematical Functions with Formulas, Graphs, and Mathematical Tables*; Dover: New York, 1965.